Atmos. Chem. Phys. Discuss., 14, 28685–28755, 2014
www.atmos-chem-phys-discuss.net/14/28685/2014/
doi:10.5194/acpd-14-28685-2014

Atmospheric Chemistry and Physics Discussions
Open Access

Interactions of bromine, chlorine, and iodine photochemistry during ozone depletions in Barrow, Alaska

C. R. Thompson[1,*], P. B. Shepson[1,2], J. Liao[3,], L. G. Huey[3], E. C. Apel[4], C. A. Cantrell[4], F. Flocke[4], J. Orlando[4], A. Fried[4,*], S. R. Hall[4], R. S. Hornbrook[4], D. J. Knapp[4], R. L. Mauldin III[4], D. D. Montzka[4], B. C. Sive[5,***], K. Ullmann[4], P. Weibring[4], and A. Weinheimer[4]**

[1]Department of Chemistry, Purdue University, West Lafayette, Indiana, USA
[2]Department of Earth, Atmospheric, and Planetary Sciences and Purdue Climate Change Research Center, Purdue University, West Lafayette, Indiana, USA
[3]School of Earth and Atmospheric Sciences, Georgia Institute of Technology, Atlanta, Georgia, USA
[4]National Center for Atmospheric Research, Boulder, Colorado, USA
[5]Institute for the Study of Earth, Oceans, and Space, University of New Hampshire, Durham, New Hampshire, USA
[*]now at: Institute of Arctic and Alpine Research, University of Colorado Boulder, Boulder, Colorado, USA

**now at: Chemical Sciences Division, Earth System Research Laboratory, NOAA, Boulder, Colorado, USA and Cooperative Institute for Research in Environmental Sciences (CIRES), University of Colorado-Boulder, Colorado, USA
***now at: National Park Service, Lakewood, Colorado, USA

Received: 30 July 2014 – Accepted: 22 October 2014 – Published: 19 November 2014

Correspondence to: C. R. Thompson (chelsea.r.thompson@colorado.edu)

Published by Copernicus Publications on behalf of the European Geosciences Union.

Abstract

The springtime depletion of tropospheric ozone in the Arctic is known to be caused by active halogen photochemistry resulting from halogen atom precursors emitted from snow, ice, or aerosol surfaces. The role of bromine in driving ozone depletion events (ODEs) has been generally accepted, but much less is known about the role of chlorine radicals in ozone depletion chemistry. While the potential impact of iodine in the High Arctic is more uncertain, there have been indications of active iodine chemistry through observed enhancements in filterable iodide, probable detection of tropospheric IO, and recently, detection of atmospheric I_2. Despite decades of research, significant uncertainty remains regarding the chemical mechanisms associated with the bromine-catalyzed depletion of ozone, as well as the complex interactions that occur in the polar boundary layer due to halogen chemistry. To investigate this, we developed a zero-dimensional photochemical model, constrained with measurements from the 2009 OASIS field campaign in Barrow, Alaska. We simulated a 7 day period during late March that included a full ozone depletion event lasting 3 days and subsequent ozone recovery to study the interactions of halogen radicals under these different conditions. In addition, the effects of iodine added to our base model were investigated. While bromine atoms were primarily responsible for ODEs, chlorine and iodine were found to enhance the depletion rates and iodine was found to be more efficient per atom at depleting ozone than Br. The interaction between chlorine and bromine is complex, as the presence of chlorine can increase the recycling and production of Br atoms, while also increasing reactive bromine sinks under certain conditions. Chlorine chemistry was also found to have significant impacts on both HO_2 and RO_2. The results of this work highlight the need for future studies on the production mechanisms of Br_2 and Cl_2, as well as on the potential impact of iodine in the High Arctic.

ACPD
14, 28685–28755, 2014

1 Introduction

The importance of halogen chemistry in Polar Regions has been well established over the past few decades since the observation of near-surface boundary layer ozone depletion in the 1980's (Oltmans and Komhyr, 1986; Barrie et al., 1988; Bottenheim et al., 1990). Since that time, ozone depletion events (ODEs) have been observed at numerous Arctic and Antarctic locations (e.g., Bottenheim et al., 2002; Saiz-Lopez et al., 2007b; Simpson et al., 2007; Oltmans et al., 2012). ODEs are characterized by episodic depletions of tropospheric ozone from background mole ratios of approximately 35 parts per billion by volume (ppbv) to less than 2 ppbv over periods of hours to days. These events are known to occur following the onset of polar sunrise, and continue through polar spring, when temperatures are low and snow and sea ice are still present, with a stable atmospheric boundary layer (Simpson et al., 2007).

Photochemical reactions involving halogen radicals, notably bromine, are thought to be the primary cause of ODEs (see Simpson et al. (2007) for a review). The chemical destruction of O_3 by Br can be described by Reactions (R1)–(R3) (Platt and Hönninger, 2003).

$$Br_2 + h\nu \rightarrow 2Br \quad \text{(R1)}$$

$$Br + O_3 \rightarrow BrO + O_2 \quad \text{(R2)}$$

$$BrO + BrO \rightarrow Br_2 + O_2 \quad \text{(R3)}$$

The efficiency of Br atoms in destroying ozone is due primarily to its relative lack of atmospheric sinks, and thus its relatively high gas-phase concentration, as well as its ability to recycle and regenerate from temporary sink species. Bromine atoms do not react appreciably with methane or other saturated hydrocarbons; thus, its primary sinks (other than O_3) consist of a few oxygenated volatile organic compounds (OVOCs) (e.g., aldehydes) or unsaturated hydrocarbons, which result in production of HBr, and HO_x species. BrO can react to regenerate a Br atom (via Reaction (R3), followed by R1), or react with HO_2 to produce HOBr, which can in turn lead to the production of two

ACPD
14, 28685–28755, 2014

Br atoms through a heterogeneous reaction mechanism termed the bromine explosion (Tang and McConnell, 1996; Vogt et al., 1996), as shown below.

$$BrO + HO_2 \rightarrow HOBr + O_2 \quad (R4)$$

$$HOBr_{(g)} \rightarrow HOBr_{(aq)} \quad (R5)$$

$$HOBr_{(aq)} + Br^-_{(aq)} + H^+_{(aq)} \rightarrow Br_{2(aq)} + H_2O \quad (R6)$$

$$Br_{2(aq)} \rightarrow Br_{2(g)} \quad (R7)$$

The production of Br_2 can thus be sustained on saline snow, ice, and aerosol surfaces, as has been confirmed in laboratory studies that have observed production of Br_2 and BrCl from aqueous and frozen halide surfaces exposed to HOBr (Fickert et al., 1999; Adams et al., 2002; Huff and Abbatt, 2002), as well as in a recent field-based study that observed Br_2 production from sunlit snowpacks in Barrow, Alaska (Pratt et al., 2013).

The presence of chlorine chemistry in the Arctic has been well recognized through indirect measurements of hydrocarbons (Jobson et al., 1994; Ariya et al., 1998; Keil and Shepson, 2006; Tackett et al., 2007) and through detection of photolyzable chlorine species (defined as $[Cl_2 + HOCl]$) (Impey et al., 1997); however, few direct measurements of chlorine species have been reported. The only currently reported measurements of ClO were by Tuckermann et al. (1997), who detected ClO at Spitsbergen. Unlike bromine, chlorine radicals efficiently oxidize a wide-range of pollutants and volatile organic compounds (VOCs), often with faster rate coefficients than analogous reactions by the hydroxyl radical (OH); thus, chlorine has an abundance of atmospheric sinks. Estimates of polar region Cl atom concentrations using hydrocarbon decay methods are typically in the range of 10^4–10^5 molecules cm^{-3} (Jobson et al., 1994; Ariya et al., 1998; Boudries and Bottenheim, 2000), approximately 2–3 orders of magnitude lower than analogous estimates of Br (Cavender et al., 2008).

Like bromine, chlorine can react directly with O_3, generating a ClO radical via Reaction (R8). The presence of ClO may also promote bromine-induced depletion of O_3 through the fast cross-reaction of BrO and ClO that serves to regenerate Br atoms

ACPD
14, 28685–28755, 2014

(Reaction R9) (Le Bras and Platt, 1995; Platt and Hönninger, 2003).

$$Cl + O_3 \rightarrow ClO + O_2 \quad (R8)$$

$$BrO + ClO \rightarrow Br + OClO \text{ (or } Cl + O_2) \quad (R9)$$

Due to analytical challenges, few tropospheric observations of Cl_2 and ClO exist, therefore the role of Cl in ozone depletion events remains uncertain and has been much debated. Typical estimated Cl concentrations are likely too low for chlorine to be a significant direct contributor to ozone depletion. However, elevated levels of Cl_2 (exceeding 100 pptv) were recently observed during the Ocean–Atmosphere–Sea Ice-Snowpack (OASIS) 2009 campaign in Barrow, Alaska using chemical ionization mass spectrometry (CIMS) (Liao et al., 2014). The impact that such high levels of Cl_2 could have on ODEs or on the oxidation chemistry of the Arctic troposphere has not been fully investigated. Although Reaction (R9) can act to enhance the rate of ozone depletion by propagating the Br cycle, formaldehyde, propanal, acetaldehyde and HO_2 are all produced as by-products of VOC oxidation by Cl and are efficient sinks for Br or BrO radicals (Shepson et al., 1996; Sumner et al., 2002). Therefore, it is likely that the interaction between chlorine and bromine is complex. Modeling studies simulating ozone depletion events often use BrCl as the primary source of Cl atoms (Calvert and Lindberg, 2003; Piot and Von Glasow, 2008), and thus [Cl] is quite low and often insignificant. Few have added significant Cl_2 sources (Sander et al., 1997; Piot and von Glasow, 2009). As a result, our understanding of chlorine chemistry in the Arctic is limited.

Iodine may play a significant role in the photochemical reactions leading to ODEs (Sander et al., 1997; Saiz-Lopez et al., 2007b, 2008; Mahajan et al., 2010) based on recent ground-based and satellite observations of IO of up to 20–50 pptv over snow and ice-covered surfaces in coastal Antarctica (Saiz-Lopez et al., 2007a, b; Schönhardt et al., 2008; Frieß et al., 2010). Although IO has been routinely detected at high levels in Antarctica, there has been no successful set of IO measurements in the High Arctic to date. However, this is possibly due to limitations of current analytical methods rather than an absolute absence of iodine chemistry. Several studies in the Arctic have

ACPD
14, 28685–28755, 2014

indicated the presence of iodine species through measurements of springtime peaks in filterable iodine (Sturges and Barrie, 1988; Barrie et al., 1994; Sirois and Barrie, 1999) and total gaseous iodine (Martinez et al., 1999). Hönninger (2002) was able to detect IO during only one instance above the detection limit at Alert in 2000 using long path DOAS, corresponding to 0.7 pptv of IO if averaged over the 10 km light path. Mahajan et al. (2010) also observed up to 3.4 pptv IO at the sub-Arctic location of Kujjuarapik, Canada. Most recently, I_2 at levels ≤ 0.5 pptv have been observed by our research group at Barrow, Alaska by CIMS, lending direct evidence supporting the presence of at least low levels of iodine chemistry in the Arctic.

Due to the lack of iodine observations in the Arctic, models often omit iodine chemistry when simulating ODEs. However, this may significantly underestimate the rate of ozone depletion because the BrO + IO cross-reaction (Reaction R10), which propagates the Br chain, has a rate constant that is approximately 2 orders of magnitude faster than the BrO self-reaction.

$$\mathrm{BrO} + \mathrm{IO} \rightarrow \mathrm{Br} + \mathrm{I} + \mathrm{O_2} \qquad \text{(R10)}$$

Indeed, previous modeling studies have found that significant enhancements in ozone depletion result from even small concentrations of reactive iodine (Calvert and Lindberg, 2004a; Saiz-Lopez et al., 2008; Mahajan et al., 2010).

Besides causing tropospheric ODEs, halogens can also impact HO_x and NO_x chemical cycles. The presence of reactive halogen species has the general effect of shifting the $[HO_2]/[OH]$ ratio towards OH (Platt and Hönninger, 2003; Thomas et al., 2012), primarily through Reactions (R11) and (R12), where X can be Br, Cl, or I.

$$\mathrm{XO} + \mathrm{HO_2} \rightarrow \mathrm{HOX} + \mathrm{O_2} \qquad \text{(R11)}$$

$$\mathrm{HOX} + h\nu \rightarrow \mathrm{X} + \mathrm{OH} \qquad \text{(R12)}$$

Halogen atoms can react with formaldehyde (and higher molecular-weight aldehydes), leading to production of hydrogen halides and HO_x. Alternatively, halogen atom reaction with HO_2 can act as a HO_x sink. The inclusion of chlorine chemistry further

ACPD
14, 28685–28755, 2014

impacts the HO_x chemistry because RO_2, HO_2 and carbonyl compounds are produced as side-products of Cl oxidation of VOCs (e.g., Reactions R13–R15).

$$Cl + CH_4(+O_2) \rightarrow CH_3OO^{\bullet} + HCl \quad (R13)$$

$$CH_3OO^{\bullet} + NO \rightarrow CH_3O^{\bullet} + NO_2 \quad (R14)$$

$$CH_3O^{\bullet} + O_2 \rightarrow HCHO + HO_2 \quad (R15)$$

Halogen chemistry also generally increases the Leighton ratio ($[NO_2]/[NO]$) through conversion of NO to NO_2 via Reactions (R14) and (R16) (Platt and Hönninger, 2003).

$$XO(X = Br, Cl) + NO \rightarrow X + NO_2 \quad (R16)$$

In this work, we utilize a zero-dimensional model to further investigate the chemical interactions occurring in the Arctic related to the chemistry of halogen radicals and the interactions between bromine, chlorine, and iodine. The OASIS 2009 campaign, conducted in March and April in Barrow, Alaska, provides a valuable opportunity to perform a unique study of halogen chemistry using direct observations of a variety of atmospheric species, including HO_x and XO_x radicals, and molecular halogens, with high time resolution measured concurrently and from a single location. During OASIS, measurements of a large suite of saturated, unsaturated, and oxygenated VOCs, numerous halogenated species (e.g. Br_2, Cl_2, BrCl, HOBr, BrO, ClO), OH, HO_2, NO, NO_2, HONO, O_3, and actinic radiation were conducted. We constrain our model with time-resolved data from OASIS, in order to investigate the following questions:

- What is the fraction of ozone depleted by each halogen atom, and how does each of the halogens impact the rate and timescale of ozone depletion?
- How do chlorine and iodine impact bromine chemistry relating to ODEs?
- What is the effect of halogen species on HO_x and NO_x chemistry, and, conversely, what is the effect of HO_x and NO_x on halogen chemistry?

ACPD
14, 28685–28755, 2014

– What is the importance of chlorine chemistry (e.g., is it only the BrO + ClO cross-reaction that makes chlorine chemistry important)?

Several modeling scenarios have been constructed in an effort to address these questions and to dissect the complex chemistry occurring during ODEs. The results of this work have been organized in the following manner:

– Section 3.1: comparison of modeled vs. observed mole ratios for pertinent species.

– Section 3.2: contribution of Br, Cl, and I to ozone depletion and the rate and timescale of ozone loss.

– Section 3.3: impact of chlorine on bromine chemistry and oxidation capacity.

– Section 3.4: impact of iodine and bromine–iodine interactions.

2 Model description

The model used for this study is a zero-dimensional, photochemical model solved using the commercial software FACSIMILE. It incorporates much of the known gas-phase chemistry that occurs in the Arctic in 216 gas-phase reactions and 42 photolysis reactions (Tables 1 and 2). The model also includes deposition/uptake to snow/aerosol surfaces for certain species, aqueous phase halide reactions, (Tables 3 and 4), and a simple dilution rate for long-lived species (e.g., PAN).

The model was developed to investigate, as a particularly useful example case study, the period 25 through 31 March 2009, which included a 3 day ozone depletion event during which O_3 remained below 1 ppbv. This time period was chosen to investigate the changes in halogen interactions under different ozone regimes, i.e. background ozone (~ 30 ppbv), ozone depleting periods, full ozone depletion (< 5 ppbv), and ozone recovery, during which winds were consistently arriving at Barrow from the frozen Arctic

ACPD
14, 28685–28755, 2014

Ocean. In order to enable focused pursuit of specific questions, the model was constrained to observed values of O_3, C_2H_2, C_2H_4, C_2H_6, C_3H_8, C_3H_6, n-C_4H_{10}, i-C_4H_{10}, HCHO, CH_3CHO, CH_3COCH_3, methyl ethyl ketone, Cl_2, and CO (shown in Fig. 1), as well as calculated time-varying photolysis rate coefficients (J) for O_3 and NO_2. A summary of the ambient measurements and instrumental methods is outlined in Table 5. Observed values were incorporated at 10 min time steps over the entire 7 day period. Constraining the model with these time-varying observations precludes the need for parameterization of atmospheric transport due to advection, and thus justifies the use of a zero dimensional model for this study. It is important to note that, because our objective was to investigate the halogen chemistry occurring during this time period rather than to attempt to simulate an ozone depletion event, we have constrained our model with the observed ozone mole ratios in order to fully study the fast chemical interactions occurring under these observed conditions, which are strong functions of $[O_3]$.

Mole ratios of CH_4 were held constant at an average value for this time of 1.89 ppmv as reported by the NOAA-ESRL Barrow Observatory. $[H_2O]$ was calculated for 25 March from observed meteorological conditions of 78 % relative humidity and an ambient temperature of −19.5 °C (NOAA; Barrow airport data), corresponding to a water vapor concentration of 2.23×10^{16} molecules cm^{-3}. This was held constant throughout the simulation. Temperature was not varied in the model.

The gas-phase chemical reactions and corresponding rate constants used in the model are shown in Table 1. Unless otherwise noted, all rate constants were calculated for a temperature of 248 K, consistent with average ambient conditions in Barrow for this time (NOAA Barrow Observatory). This mechanism includes halogen, HO_x, NO_x, and VOC chemistry associated with ozone depletions in the Arctic spring. The inorganic iodine reaction scheme used here is adapted from McFiggans et al. (2000, 2002), Calvert and Lindberg (2004a), and Saiz-Lopez et al. (2008). Organic iodine compounds are not included. Although some organic iodine compounds have been observed in coastal and marine locations (Carpenter et al., 1999; Jones et al., 2010),

ACPD
14, 28685–28755, 2014

I_2 is likely the major source of atmospheric iodine (Saiz-Lopez and Plane, 2004) and, thus, was assumed to be the reactive I source in this model. It should also be noted that while I does not react appreciably with VOCs, it is likely that I/IO does react with RO_2 radicals (Sommariva et al., 2012). However, these reactions are not included here. Thus, though the iodine reaction scheme agrees with previous studies, it is likely incomplete; therefore, modeled iodine chemistry should be taken only as potential impacts to help direct future research efforts.

Photodissociation reactions included in this model are listed in Table 2. For many of the species, time-varying J coefficients were calculated using a modified version of the Tropospheric Ultraviolet and Visible (TUV) Radiation model (Madronich and Flocke, 1999) based on in situ 0.1 Hz measurements of downwelling actinic flux conducted throughout the duration of the OASIS campaign and a surface albedo of 0.8. Upwelling flux was estimated as a function of solar zenith angle assuming clear sky conditions. The sum of upwelling and downwelling radiation was used by the TUV model to calculate the total photolysis frequencies. J coefficients for solar noon on 25 March (listed as J_{max}) are provided in Table 2 as an example. J coefficients were input into the model at 10 min time steps for O_3 and NO_2. All other J values were scaled to J_{NO_2} in the modeling code.

J coefficients from OASIS were not available for OClO, HOCl, or iodine compounds. An estimate for J_{max} for OClO was taken from Pöhler et al. (2010) and that for HOCl was taken from an Arctic model study by Lehrer et al. (2004), which were then scaled to J_{NO_2}. J values for iodine compounds were calculated according to the work of Calvert and Lindberg (2004a, b), who also simulated conditions for late March in Barrow, although we note that there is a larger uncertainty for the photolysis coefficients for the iodine species, with the exception of I_2. Time-varying J coefficients for the iodine species were calculated using a fourth-order polynomial and varying the solar zenith angle from 98.4 to 72.3°.

Deposition of species to the snowpack is estimated based on measured dry deposition velocities and applied using Eq. (1) to calculate transfer coefficients (k_t) from the

ACPD
14, 28685–28755, 2014

gas to aqueous phase.

$$k_t = \frac{V_d}{h} \quad (1)$$

V_d is the dry deposition velocity (in $cm\,s^{-1}$), and h is the boundary layer height. Most previous estimates of ozone deposition velocities to snow in the Arctic range from 0 to $0.2\,cm\,s^{-1}$ (Gong et al., 1997; Helmig et al., 2007). Here, we use an average value of $0.05\,cm\,s^{-1}$ for ozone, similar to the modeling studies of Cavender et al. (2008) and Michalowski et al. (2000). However, there is large uncertainty in this parameter and often-contradictory observations from field measurements (Helmig et al., 2007, 2012). For 25 March (day 83), the boundary layer height in Barrow was estimated at 300 m based on radiosonde data and model simulations (R. Staebler, Environment Canada, personal communication, 2010). This corresponds to a k_t for ozone of $1.67 \times 10^{-6}\,s^{-1}$. Because dry deposition velocities to snow have not been determined for the halogen acids, we use the estimation method of Michalowski et al . (2000) and assume a transfer coefficient 10 times greater than that for ozone. Thus, for HBr, HCl, HOBr, HOCl, and HOI, $k_t = 1.67 \times 10^{-5}\,s^{-1}$ (Appendix A, Table A3). Similarly, we assume an equivalent deposition velocity for the oxidized acidic nitrogen compounds (i.e. HNO_3, HO_2NO_2, HONO, N_2O_5), though a full mechanism of aqueous-phase nitrate chemistry is not included in this model. Deposition coefficients for Cl_2, Br_2, and BrCl are estimated by comparison of Henry's Law constants for these compounds with those of O_3 and the halogen acids. It should be noted that this estimation is a very simplified parameterization of surface deposition. In reality, the transfer of species to the snowpack is governed by the eddy diffusivity, rate of gas diffusion through the snow (i.e. wind pumping), and efficiency of uptake by the surface. However, consideration of turbulent mixing and vertical transport requires a more sophisticated model and is outside the scope of this 0-D model study. Since we are primarily focusing on the gas-phase radical interactions in this study, and we do not calculate or draw conclusions from the production rate of molecular halogens from the heterogeneous mechanism, this simplified mechanism

ACPD
14, 28685–28755, 2014

is sufficient for the questions being pursued here, particularly given the uncertainties associated with the estimated deposition velocities. Field measurements of deposition velocities for the molecular halogens would be highly valuable to direct further modeling efforts that depend on heterogeneous chemistry.

Our model was initially developed to utilize multiphase chemistry to produce Br_2 (and Cl_2) following the method and chemical mechanism of Michalowski et al. (2000), with only slight adjustments. Transfer coefficients into and out of the particle phase were calculated as described in Jacob (2000), and the snowpack volume available for heterogeneous reaction was limited to a column 10 cm deep, based on the effective UV extinction depth for Arctic snow (King and Simpson, 2001). Constant concentrations of chloride and bromide ions in the aerosol and snowpack were used throughout the duration of the simulation, as it is likely that these represent an inexhaustible source of halide ions (Lehrer et al., 2004). Concentrations of Br^- and Cl^- in the snowpack were calculated by assuming all bromide and chloride from bulk snow measurements (Krnavek et al., 2011) were contained within the quasi-liquid layer (QLL) (Cho et al., 2002). We used a pH of 4 for the QLL as an estimate, which is in line with previous modeling studies (Thomas et al., 2011, 2012). Aerosol halide concentrations were used as reported for the bulk aerosol chloride and bromide measurements from Barrow, Alaska (Li and Winchester, 1989), and we used an estimate of H^+ for Arctic aerosols from the ARCPAC flight campaign (Fisher et al., 2011). Additionally, upward mixing of chemical species emitted from the snowpack heterogeneous reactions was simplified such that it was assumed to be limited only by vertical mixing from the surface and did not include diffusion through the snowpack interstitial air, which is dependent mostly on wind pumping (a parameter not included in this 0-D model). The mass transfer and aqueous phase reactions comprising the multiphase component of the model are shown in Tables 3 and 4.

Using this mechanism, we were able to produce sufficient gas-phase Br_2 in the model solely from the snowpack/aerosol heterogeneous reactions with aqueous bromide, however, we could not reproduce the day-to-day variability in $[Br_2]$ from only the

ACPD
14, 28685–28755, 2014

heterogeneous chemistry; thus, since our main objective was to examine interactions between halogen radical species, we used an additional prescribed, time-varying flux (input as a volumetric addition rate), ranging from 1×10^4 to 9×10^6 molecules cm^{-3} s^{-1}, to enable reasonable estimation of both the $[Br_2]$ and [BrO] observations. This was necessary to ensure that [Br] and [BrO] were accurately represented, so that we could properly examine interactions with other radicals, e.g. HO_2, ClO, and IO. Br_2 values were not read into the model as was done for Cl_2, because there is some degree of debate regarding the accuracy of the daytime Br_2 measurements (this will be discussed further in Sect. 3.1), and therefore the flux was adjusted such that BrO was well-represented. It should be noted, however, that the uncertainty in the BrO measurements is high during ODEs as the observed values are very near the detection limit (LOD of ~ 2 pptv with uncertainty of −3/+1 pptv near the LOD), and thus the uncertainty in modeled [Br] would be greatest during these periods. For Cl_2, the production mechanism is unknown, and thus it was essential to use the observed concentrations. Only daytime BrCl was used as produced in the model multiphase mechanism. BrCl measurements from OASIS are sparse, however, the daytime simulated BrCl mole ratios of 0–10 pptv are in agreement with the available observations for the campaign.

Volumetric fluxes were also introduced into the model for NO_2, HONO, and I_2 (Table 6). The fluxes of HONO, NO_x and I_2 were scaled to J_{NO_2} since HONO and NO_x (and likely I_2) are photochemically produced (Honrath et al., 1999; Zhou et al., 2001; Saiz-Lopez et al., 2011). All fluxes, with the exception of I_2, were adjusted in order to agree with observed gas-phase concentrations of the respective species. The NO_2 flux was variable, ranging from 1×10^5 to 9×10^6 molecules cm^{-3} s^{-1}. The I_2 flux was chosen such that average daytime gas-phase mole ratios of IO remain below 1 pptv (i.e., below the detection limit of DOAS and in line with previous indications of [IO] in the Arctic) for the majority of days. Only during the ozone depletion period did simulated IO reach close to 2 pptv, for the chosen I_2 flux. The higher [IO] during ozone-depleted periods is a result of the constant I_2 flux that is utilized for iodine, in contrast to bromine and chlorine species, which use actual observations. Because the I_2 flux is constant

ACPD
14, 28685–28755, 2014

during the ODE, while Br_2, and especially Cl_2 are decreased, iodine becomes more dominant for reaction with O_3 and IO increases. $[I_2]$ averages ~ 0.02 pptv throughout the simulation. These levels enabled us to examine the potential impact of even small concentrations of I and IO.

3 Results and discussion

3.1 Comparison of modeled and observed mole ratios for select species

Those species that are not specifically prescribed in the model (e.g. all radical species and many inorganic halogen compounds) by inputting time-varying observations or by introducing a flux are allowed to freely evolve. Here we compare modeled vs. observed mole ratios for only those species that are most important for this analysis on halogen interactions.

Since the contribution of each halogen atom to ozone destruction is a function of its concentration, it is important that the model simulates halogen radicals at levels that are consistent with observations. Comparisons of the multi-day model output with observed BrO and ClO are shown in Fig. 2d and e. ClO observations are limited, but the model captures the occurrence and general shape of the ClO peak observed on 29 March. However, the model generally under predicts [ClO] where there are available observations. A question to address is the extent to which there are other sources of Cl atoms during this time, such as HOCl or chlorinated organic compounds that are not included here. In Fig. 2d, the modeled BrO output generated through the varying Br_2 flux is compared with BrO observations. The model represents the overall temporal profile and magnitude of [BrO] throughout this period. This is important for the analysis of the interactions between BrO, ClO, and IO, which is the focus of this work. To produce the amount of BrO necessary to match observations, and especially for 29 and 30 March (a period of higher $[NO_2]$ and [BrO]) additional surface fluxes of Br_2 (up to 9×10^6 molecules cm^{-3} s^{-1}) had to be added to the model, which resulted in daytime

ACPD
14, 28685–28755, 2014

[Br_2] ranging from 2–12 pptv (Fig. 2a). It has been suggested that daytime Br_2 observed by CIMS contains a contribution from HOBr conversion to Br_2 on the inlet, and that daytime Br_2 was below detection limits on average due its fast photolysis rate (Liao et al., 2012). However, this modeling study suggests that Br_2 should indeed be present in the daytime (given observed [BrO]), though it is acknowledged that there is some degree of interference from HOBr, as is apparent from the model under-prediction of Br_2 on 31 March. Considering an *e*-folding photolytic lifetime of Br_2 at solar noon of 23 s ($J_{max} = 0.044\,s^{-1}$), and using the method of Guimbaud et al. (2002), the effective daytime mixing height (Z^*) of Br_2 in the stable air typical of the Arctic ($K_c = 95\,cm^2\,s^{-1}$) is ~ 0.5 m. Assuming simple first-order kinetics, the [Br_2] remaining after mixing up from the surface to the intake of the CIMS (~ 1 m or 2 lifetimes) is 10 % that at the surface. A recent study examining Br_2 production from surface snow in Barrow demonstrates that enhanced Br_2 production is observed in the presence of solar radiation (Pratt et al., 2013). Given that the Br_2 concentrations in the snowpack interstitial air should be elevated due to heterogeneous production mechanisms (e.g., the bromine explosion), and that production should be greater during sunlit periods, it seems reasonable to conclude that Br_2 should sometimes be observable during the day. Indeed, Br_2 mole ratios needed in the model to reproduce BrO observations agree with the "uncorrected" Br_2 observations (shown as the red data in Fig. 2a), as reported in Liao et al. (2012).

Figure 2b and f compare the model output for Br and Cl atom concentrations (black trace) with steady-state approximations of [Br] and [Cl] following the method of Stephens et al. (2012), as direct observations of Br and Cl atoms have not yet been achieved. In both cases, the model-simulated output is greater than the steady-state approximations on a few days, sometimes by as much as 90 %, although both methods capture the diurnal trends and fluctuations. A notable feature of Fig. 2b is the rather high Br atom concentrations during the three day ODE, with concentrations up to 2×10^9 molecules cm^{-3} (~ 67 pptv), though as mentioned previously, this should be considered an upper limit due to the uncertainty of the BrO measurements and the potentially positive model bias during this time. Nonetheless, higher [Br] (and [I]) is ex-

ACPD
14, 28685–28755, 2014

pected during periods of complete ozone depletion due to the loss of this dominant Br atom chemical sink, however, these concentrations are on the high end of previous estimates using hydrocarbon measurements, which range from 1×10^6 to 1×10^9 for ODEs (Jobson et al., 1994; Ariya et al., 1998; Rudolph et al., 1999). While [Br] peaks during periods of low O_3, [Cl] is enhanced when O_3 is present due to the elevated Cl_2 mole ratios that are observed only when O_3 is above ~ 10 ppbv (Fig. 1a). The model predicts Cl atom concentrations of 2×10^5 to 6×10^5 molecules cm^{-3}, which is also higher than previous estimates of 1×10^3 to 1×10^5 determined from hydrocarbon measurements (Jobson et al., 1994; Ariya et al., 1998; Rudolph et al., 1999; Boudries and Bottenheim, 2000; Keil and Shepson, 2006). As discussed in Stephens et al. (2012), the hydrocarbon-based methods average over the transport path, which can be aloft, and thus should be lower than that observed near the surface, if the surface is the Cl_2 and Br_2 source.

NO_2 mole ratios in Barrow are often quite variable and relatively high compared to other polar measurement locations (Beine et al., 2002). At times, winds travel from the southwest direction, bringing air influenced by Barrow emissions over the measurement site. This is the case for the high NO_2 observed at the beginning of 25 March, which correlates to enhanced CO. To simulate this, the model was initialized with a very high NO_2 concentration (1×10^{11} molecules cm^{-3}), which was quickly depleted via photochemical conversion (Fig. 2g). 29 and 30 March showed an enhancement in measured NO_2, as well; however, the wind direction was easterly (i.e. from the sea ice) and there was no concomitant increase in CO for this period. In order to capture the general temporal profile of the majority of the data during this period, an increase in the surface flux of NO_2 (up to 5×10^6 molecules cm^{-3} s^{-1}) was required. The modeled [NO_2] does not contain the sporadic high spikes of NO_2 shown in the observations (as it is possible that these spikes were due to intermittent local contamination, e.g. generators or vehicles at the base), nor the high nighttime values observed on 29–30 March; however, it does capture the trend of the majority of the data for this period.

ACPD
14, 28685–28755, 2014

Model simulations of [OH] and [HO_2] (Fig. 2h and i) lie within the bounds of measurement uncertainty for the ambient data, with the exception of 29 March when the model under predicts HO_2 by factor of ~ 3. The accurate simulation of OH and HO_2 is important since halogen chemistry, especially that involving chlorine, can have a significant impact on the HO_x budget. The discrepancy between the modeled and observed HO_2 for 29 March may lead to a less than realistic impact of HO_2 on oxidation chemistry for this day. The model captures the temporal cycle of HOBr well; however, it generally over predicts the daytime peak mole ratios (Fig. 2c). It is unclear why this should be the case, given that both BrO and HO_2 are well-represented. This suggests that either our simple parameterization of deposition to snow and particle surfaces is slower than that occurring in nature, or that we are missing some other important HOBr sink.

3.2 Contribution of Br, Cl, and I to ozone depletion and the rate and timescale of ozone loss

An important question regarding ozone depletion events is the contribution of the halogen radicals, Br, Cl, and I, to the total destruction of ozone and the rate of ozone depletion. Based on field measurements of reactive bromine compounds, primarily BrO, it is generally accepted that bromine is the dominant reactant leading to ozone destruction (Simpson et al., 2007). However, this has not been quantified, nor has this been investigated for varying chemical conditions. Few studies have examined the impact of Cl on ozone depletion, and these have not had the benefit of in situ observations of Cl_2 and ClO with which to compare their models. This observational data set and model thus represents a unique opportunity.

In this study, "Base Model" runs are those that include both bromine and chlorine. "Br Only" simulations are performed by removing Cl_2. Simulations with iodine are conducted by introducing a flux of I_2 of a magnitude necessary to keep the average daytime [IO] $\leq$ 1 pptv (i.e., less than the typical LOD of the LP-DOAS, but of a magnitude comparable of that observed by Hönninger, 2002). Additional sensitivity studies are presented that include an increased I_2 flux such that 0.5 pptv of I_2 is present, which is

ACPD
14, 28685–28755, 2014

consistent with an upper limit of recent I_2 observations in Barrow. Under the conditions of this study, this leads to approximately 5–6 pptv of IO. The simulated IO and I atom mole ratios for the studied period for the 1 ppt IO scenario are shown in Fig. 3. It is important to note that the model is adjusted to fit observations using the Base Model only. No re-adjustments are made to the model when either Cl_2 is turned off, or when I_2 is turned on, in order to observe the effect of a one variable change.

The time-varying fraction of ozone depleted by bromine, chlorine, and iodine was calculated by considering those reactions that destroy ozone (i.e. Reaction (R2) for Br and the analogous reactions for Cl and I) while correcting for those reactions that result in the regeneration of O_3. Here, photolysis of BrO, ClO, or IO, as well as reaction of XO with NO, ultimately lead to O_3 production. The rate of O_3 loss by halogen X is determined by Eq. (2), where X = Br, Cl, or I, and the total chemical O_3 loss rate is calculated using Eq. (3). The fractional contribution for each halogen is then determined by dividing the two quantities.

$$\text{Rate of } O_3 \text{ loss by } X = k[X][O_3] - k[XO][NO] - J[XO] \quad (2)$$

$$\begin{aligned}\text{Total } O_3 \text{ loss rate} = {} & k[Br][O_3] + k[Cl][O_3] + k[I][O_3] + k[O(^1D)][H_2O] \\ & + k[OH][O_3] + k[HO_2][O_3] - k[BrO][NO] - J[BrO] - k[ClO][NO] \\ & - J[ClO] - k[IO][NO] - J[IO]\end{aligned} \quad (3)$$

While we recognize that considering only the sum of the rates of XO + XO reactions (where X = Br, Cl, or I) has generally be used in previous studies to estimate the rate of ozone destruction (Le Bras and Platt, 1995; Platt and Janssen, 1995), we have chosen to use Eqs. (2) and (3) as it is likely that these complex interactions are oversimplified by the XO + XO method. Indeed, we show in a forthcoming manuscript (Thompson et al., 2014, Bromine atom production and chain propagation during springtime Arctic ozone depletion events in Barrow, Alaska) that the XO + XO method underestimates chemical ozone loss by Br and Cl atoms when compared to Eq. (2).

Figure 4 shows the fraction of the rate of O_3 depletion by Br and Cl for the Base Model (panel a) and with iodine included (panel b) as a diurnal average for only 25

ACPD
14, 28685–28755, 2014

and 29–30 March, for conditions in which O_3 is > 5 ppbv, since this quantity is only meaningful when O_3 is present. Br accounts for the vast majority of O_3 depletion, from 75–95 %, whereas Cl only accounts for 5–10 % of ozone loss on average. In panel b it can be seen that the low levels of iodine considered (1 ppt IO) contribute more to O_3 destruction than does chlorine on average, with a contribution up to 40 %. This is true also when considering just 29 and 30 March, a period during which $[Cl_2]$ reached up to 100 pptv. Thus, it is clear that even low levels of iodine (Fig. 3) can have a significant contribution to ozone depletion.

To investigate this in further detail, we used a focused version of our model that simulated a 1.5 h period using just mid-day conditions to facilitate instantaneous calculations of ozone depletion. We used chemical mole ratios similar to those of 25 March (the first day of the period) as an example day that represents approximately average Br_2 and Cl_2 levels observed during the campaign (at up to ∼ 4 and ∼ 16 pptv, respectively) and ozone at near background concentrations. The mid-day version of our model was run with constant molecular halogen and VOC concentrations, thus, although the conditions are similar to 25 March, the results are not directly comparable. Although the remnants of the NO_x plume are observable in the ambient data during the mid-day hours, the simulated NO_2 is at typical levels in this model (∼ 8 pptv), the halogen radical species are well represented and O_3 is constrained to observed mixing ratios. Thus, the variability seen in the ambient NO_x data is not represented or tested in this analysis.

The fractional contribution of each halogen to ozone destruction was calculated using Eq. (4) for five different model scenarios with different combinations of halogens present: Br Only, Br and Cl (the Base Model), Br and I (1 pptv IO), Br, Cl and I (1 pptv IO), and Br, Cl and I (0.5 pptv I_2). Values of Br_2, Cl_2 and I_2 used for 25 March were 4, 16 pptv, and 0.02 pptv, respectively. In Eq. (4), P, Q, and R represent the total value for model "counters" for each process in parentheses, and the denominator is

ACPD
14, 28685–28755, 2014

the molecules cm^{-3} of O_3 destroyed over the simulated period.

$$F_X = \frac{P(X + O_3) - Q(J_{XO}) - R(XO + NO)}{-\Delta[O_3]} \quad (4)$$

Results of this calculation are shown in Table 7 for the five scenarios studied.

It is clear from Table 7 that Br is the primary driver of O_3 loss with at least 70 % contribution in all cases, reaching up to 93 % in the Base Model. In comparing the "Br Only" run with the "Br and Cl" run, one can see that while Cl does not directly deplete O_3 significantly (due to its much lower concentration), it does enhance the O_3 depletion caused by bromine, with the fraction of ozone depleted by Br increasing from 91 % in the Br Only scenario to 93 % in the Br and Cl scenario. This is primarily a result of the efficient cross-reaction between BrO and ClO that regenerates Br and thereby increases the [Br]/[BrO] ratio. Comparing "Br Only" with "Br and I", it is apparent that iodine chemistry directly contributes a significant amount to ozone depletion, at a fractional contribution of 15 % with just 1 ppt IO present, due to both the fast reaction between I and O_3 and IO and BrO, as well as the lack of known competing sinks for I. From examination of the fractional ozone depletion, it appears that iodine chemistry decreases the Br-destruction of ozone; however, on an absolute basis, there is an increase in the total number of ozone molecules per cm^3 destroyed by Br in the "Br and I" simulation (1.63×10^{11} molecules cm^{-3} O_3 destroyed) compared to the "Br Only" simulation (1.30×10^{11} molecules cm^{-3}), as well as an increase in total ozone lost by a factor of 1.5 for the integrated 1.5 h simulation period. When 0.5 pptv of I_2 is included at a constant level the base model, there is a factor of 1.9 increase in total O_3 lost, with iodine contributing 22 % to the ozone depletion. The absolute ozone destruction by Br is enhanced more by iodine than by chlorine as a result of the very fast reaction between BrO and IO. Therefore, while Cl acts primarily to enhance Br chemistry, I both increases the efficiency of bromine catalyzed ozone destruction, and directly depletes ozone. The presence of Br, Cl, and I results in the greatest total ozone loss for this simulated period. The last row of Table 7 shows the total O_3 destruction for the simu-

ACPD
14, 28685–28755, 2014

lation period. It is clear that fully understanding ODE chemistry will require a complete understanding of all three halogen radical families.

Platt and Janssen (1995) indicate that ~ 99 % of Br atoms react with O_3 when present at background levels, while only ~ 50 % of Cl atoms react with O_3 due to efficient reactions with many VOCs. However, this quantity is highly dependent on the mole ratios of O_3, HCHO, CH_3CHO, and the VOCs, which can fluctuate independently of each other. To further investigate how the three halogens contribute to ozone depletion, we considered the fraction of available Br, Cl, and I atoms that react with O_3 over all other competing pathways across the seven-day simulation with iodine included (at 1 pptv IO) as shown in Fig. 5. The inclusion of iodine does not significantly change the result for Br and Cl, thus only the simulation including I is shown. Br atoms were simulated to react with O_3 75–95 % of the time when O_3 is not depleted, but this fraction fluctuates significantly and is at times below 50 % when O_3 is depleted (i.e., < 5 ppbv). Cl atom reaction with O_3 varies between 10–20 % on average, and is always less than 30 % for this time period. These numbers are lower than those estimated previously, likely because we are using actual measurements of all of the known Br and Cl atom sinks that contribute to this quantity, e.g. HCHO, CH_3CHO, VOCs and NO_x. Based on our chemical mechanism, I atoms can react with O_3 up to 100 % of the time, and usually up to 90 %, consistent with the estimates of Platt and Janssen (1995), who determined 99 % for I. However, as stated previously, it is likely that our iodine reaction scheme is incomplete, e.g. for IO reaction with peroxy radicals.

Not all halogen atom reactions with O_3 result in a net loss of ozone. Though up to 90 % of Br atoms react with O_3, most of these reactions do not ultimately destroy ozone as it can be reformed via e.g., BrO photolysis or BrO reaction with NO. When considering only Br and Cl in our mid-day model, 70 % of the BrO formed regenerates O_3 through photolysis or reaction with NO, whereas this quantity is only 12 % for ClO, which photolyzes much more slowly. While this suggests that Cl atoms are actually more efficient at destroying ozone on a per atom basis, the lower concentration of Cl due to the numerous competing Cl-atom sinks make it a minor player in ozone deple-

ACPD
14, 28685–28755, 2014

tion. When iodine is included at 1 pptv IO, thus opening the BrO + IO cross-reaction, the percentage of BrO that reforms O_3 drops to 64 % and that for IO is comparable at 65 %.

It is useful to also consider the rate of ozone depletion. Often, fast apparent ozone depletions, in which O_3 is observed to decrease over timescales of hours, have been attributed to air mass transport of ozone-depleted air, whereas local chemistry is believed to result in a more gradual depletion (Bottenheim and Chan, 2006; Simpson et al., 2007; Halfacre et al., 2014). The ozone depletion rate and the resulting timescale for depletion induced by Br, Cl, and I, both in isolation and when allowed to interact was investigated with modeling runs conducted for "Br Only", "Cl Only", and "I Only", as well as with different combinations of the above, including a simulation with 0.5 pptv I_2. Here, we considered only the instantaneous ozone depletion rate at mid-day of 25 March, determined using Eq. (3) and averaged over 1 h of simulation time, to calculate the depletion timescale. Table 8 shows the resulting ozone depletion rates in ppbv h^{-1} for the different permutations of halogen radicals studied, along with the resultant timescale for total ozone depletion from a background of 30 ppbv (assuming a constant ozone depletion rate, which represents an upper limit as the rate of ozone depletion decreases as $[O_3]$ decreases).

For the chemical conditions observed on this day, bromine chemistry alone is capable of depleting ozone on a timescale of 9.3 h at a rate of 3.2 ppbv h^{-1}, whereas chlorine chemistry at the levels observed for this day (16 pptv Cl_2) would require 30 days at a rate of 0.04 ppbv h^{-1}. Iodine alone at 1 pptv IO depletes ozone at a rate of 0.8 ppbv h^{-1} in 1.6 days. Of note is the apparent synergy that exists between the halogens. That is, the combination of any halogen species depletes ozone at a faster rate than the sum of the components run in isolation. This is a result that was previously found for the interaction of bromine and iodine in modeling studies by Calvert and Lindberg (2004a, b), Saiz-Lopez et al. (2008) and Mahajan et al. (2010). The greatest ozone depletion rate of 6.6 ppbv h^{-1}, with a timescale for complete depletion of only 4.5 h, results when all three halogens are present, with I_2 set at 0.5 pptv. Based on

ACPD
14, 28685–28755, 2014

these results, it can be concluded that iodine has the potential to have a much greater impact on ozone depletion than chlorine. Low levels of iodine (1 ppt IO) increase the ozone depletion rate by a factor of 1.6 over the Br only run, whereas the addition of Cl only increases the ozone depletion rate by another 3 %.

It should be noted, however, that the ozone lifetimes discussed above simply represent the calculated ozone lifetime, as determined from measurements conducted within the surface layer. As discussed in detail in Tackett et al. (2007), the current view of the boundary layer is one that is very chemically stratified, with the most important source of Br_2 and Cl_2 likely from the snowpack surface. Thus, the concept of "boundary layer" is one that has been defined in terms of the height over which ozone is observed to be depleted, i.e. typically ~ 400 m (Bottenheim et al., 2002; Helmig et al., 2012). It is likely, however, that ozone is depleted largely in the very near surface layer, and the time scale for that depletion is thus determined in significant part by the time scale for downward diffusion of ozone in the 0–400 m range to the near-surface layer in which BrO_x concentrations are large. In short, when averaged over the entire boundary layer, the actual ozone depletion timescale may potentially be slower than that calculated here using only surface measurements.

A highly significant finding from the OASIS 2009 campaign was the observation of unexpectedly high levels of Cl_2 (Liao et al., 2014). Given the observed [Cl_2] maxima of 100–400 pptv, a sensitivity study was performed to investigate the impact that such high concentrations could have on ozone depletion chemistry. Again, we considered only the conditions of mid-day of 25 March for this study and determined the average ozone depletion rate (using Eq. 3) across 1 h of the simulation period for four different scenarios performed by varying the [Cl_2]. [Cl_2] was varied with mole ratios of 16 (Base Model), 100, 250, and 400 pptv. Br_2 was present in these simulations at the same concentration (~ 4 pptv) as used in the Base Model. The rate of ozone depletion and timescale for depletion resulting from the various [Cl_2] is shown in Table 9. The presence of 100 pptv of Cl_2 shortens the timescale for total depletion from 8.7 h (for 16 pptv Cl_2) to 6.6 h. For comparison, the Base Model with I_2 (at 1 pptv IO, 0.02 pptv I_2), as

ACPD
14, 28685–28755, 2014

shown in Table 8, has an ozone depletion timescale of 5.6 h. Thus, the presence of only 0.02 pptv of I_2 has a greater effect on the ozone depletion rate than does 100 pptv of Cl_2. 400 pptv Cl_2 is an extreme event, though close to the maximum Cl_2 observed during OASIS, and the resultant ozone depletion timescale from 30 ppbv is only 2.1 h. Our modeling results do not show indications of a "chlorine counter-cycle" hindering ozone depletion as suggested by Piot and von Glasow (2009).

Although the depletion timescales reported here, both for base model conditions and for elevated [Cl_2], represent relatively fast ozone depletion and, as stated, represent an upper limit assuming a constant ozone depletion rate, total ozone depletions are often observed to occur on timescales of a day or less (Tang and McConnell, 1996; Simpson et al., 2007), and a fast ozone depletion of ~ 7 h attributed to local chemistry was reported over the Arctic Ocean by Jacobi et al. (2006). Thus, the ozone depletion rates calculated here (including for elevated [Cl_2]) show that rapid photochemical ozone depletion events are possible, and thus one should not assume that all fast ODEs represent transport, without appropriate supporting information. Back-trajectories for periods of very high [Cl_2] during OASIS indicate air mass transport over the surface of the Arctic Ocean (Stephens et al., 2012). Ozone instruments on-board the O-Buoy network of sea ice-tethered buoys (Knepp et al., 2010) in the Arctic Ocean have also indicated very fast ozone depletions, with a median timescale of 10.4 h and numerous individual events much faster than that (Halfacre et al., 2014). Unfortunately, we are limited by a lack of Cl_2 measurements from across the frozen Arctic Ocean, and thus, it is not possible to speculate how widespread this elevated Cl_2 may be.

3.3 The impact of chlorine on ozone depletion chemistry and oxidation capacity

One of the primary objectives of this work was to assess the impact of chlorine on bromine chemical cycles relating to ODEs in light of the recent discovery of unexpectedly high [Cl_2] in Barrow during OASIS. We discussed the contribution of observed levels of chlorine to ozone depletion in Sect. 3.2 and the impact of varying concentrations of Cl_2 on the rate and timescale of ozone depletion. These results show that

ACPD
14, 28685–28755, 2014

chlorine itself plays only a minor role in the direct destruction of ozone until Cl_2 reaches over 100 pptv. That Cl atoms do not directly contribute significantly to ozone depletions is not surprising, given their lower ambient concentration compared to Br (see Fig. 2), due to the multitude of Cl atom sinks. In the model, the rate of Cl atom production from Cl_2 and BrCl (assumed to be surface emitted species) is also on average only 20 % of the rate of Br production from Br_2 and BrCl. The Br/Cl ratio for the Arctic has been estimated to range from 80 to 1200 when ozone is not fully depleted (Jobson et al., 1994; Keil and Shepson, 2006; Cavender et al., 2008) based on observations of halocarbons and hydrocarbon decay. Our model predicts daytime Br/Cl ratios for non-O_3 depleted days ranging from a low of 18 up to 1300, consistent with previous estimates. When ozone is fully depleted (i.e., < 5 ppbv), [Br] becomes much greater than [BrO], due to the loss of its primary atmospheric sink and the resultant lack of production of BrO, and the Br/Cl ratio increases dramatically to 8×10^3–2.5×10^5. During these periods when the ozone concentration is low, CH_3CHO becomes an important Br atom sink, with a rate of reaction with Br comparable to that of $Br + O_3$ (Fig. 6). This supports the hypothesis by Shepson et al . (1996) that aldehydic compounds, including CH_3CHO, represent important Br sinks during ODEs. HCHO is at times a major Br atom sink, but only when ambient concentrations are high enough to compete with CH_3CHO (e.g., towards the second half of 28 March where $[HCHO]/[CH_3CHO] =\sim 0.8$). Interestingly, NO_2 also represents a major Br sink during ODEs. In comparison to other Arctic locations, Barrow can have relatively high NO_x, and thus NO_2 would likely not be as important a Br sink in more pristine Arctic environments. A detailed study into the impact of these increased NO_x levels in Barrow is the subject of a forthcoming manuscript (Custard et al., 2014, The NO_x dependence of halogen chemistry in the Arctic atmospheric boundary layer), and thus is not discussed extensively here.

Although Cl chemistry can generate HCHO and CH_3CHO in the gas phase through oxidation of methane and ethane, respectively (e.g., Reactions R13–R15), it is likely not the case that these important Br sinks are the result of such reactions during ODEs. From the time series of ambient Cl_2 observations (Fig. 1a), and as discussed in Liao

ACPD
14, 28685–28755, 2014

et al. (2014), it is apparent that substantial mole ratios of Cl_2 are only observed when O_3 and radiation are present. When O_3 is fully depleted during 26–28 March, Cl_2 is nearly absent. Moreover, the efficiency of production of HCHO and CH_3CHO is NO_x-dependent, with hydroperoxide production more important at low NO_x levels typical of more remote Arctic environments. Thus, while some significant gas-phase production of HCHO and CH_3CHO can occur if [Cl] is high (Sumner et al., 2002), it is far more likely that in the Arctic, surface concentrations of these compounds are primarily derived from snowpack emissions (Grannas et al., 2007; Barret et al., 2011). The production of HCHO and CH_3CHO from the snowpack has been documented in previous studies (Sumner and Shepson, 1999; Grannas et al., 2002) and strong vertical fluxes of both compounds were observed during OASIS (Barret et al., 2011; Gao et al., 2012).

Based on the reaction scheme shown in Reactions (R13)–(R15), and similar VOC oxidation pathways involving Cl atoms, Cl chemistry can also generate HO_2, a very significant BrO sink (though relatively unimportant for Br atoms) and an important atmospheric oxidant; however, this too is dependent on NO_x. It has been suggested that the presence of chlorine will significantly increase HO_2 (Rudolph et al., 1999; Piot and von Glasow, 2009). Figure 7 presents results of a sensitivity study in which simulations with different combinations of halogens present were performed to investigate the impact on HO_2. For days when O_3 is not fully depleted (i.e., 25, 29, and 30 March), and when Cl_2 is present, the "Cl Only" simulation results in HO_2 concentrations up to 1×10^8 molecules cm^{-3} (~ 3.4 pptv) for [Cl_2] nearing 100 pptv (29 and 30 March). For 30 March, the "Cl only" and "Br only" simulations indicate comparable HO_2 concentrations. However, the "Br Only" simulation results in greater [HO_2] for 25 and 29 March than does "Cl Only." Generally, the greatest [HO_2] is produced in the Base Model when both Br and Cl are present, although in some cases, specifically when O_3 is depleted (and thus Cl_2 is absent as discussed above) HO_2 is indistinguishable from a Br-only case. During the 26–28 March period, there would be little HO_x production from O_3 photolysis, and as Cl_2 is also nearly absent, bromine chemistry is the primary source of HO_x production.

ACPD
14, 28685–28755, 2014

To investigate this further, time-varying rates of production of OH and HO_2 were determined from their primary source reactions (Fig. 8). Under our modeling conditions for the 7 days studied, when O_3 is not fully depleted, HO_x is produced primarily through photolysis of HONO (as postulated by Zhou et al., 2001 and Villena et al., 2011) and as a by-product of Br reaction with HCHO (blue and pink traces in Fig. 8), with significant production from photolysis of HCHO, as well, confirming the importance of snowpack-emitted carbonyl compounds for the oxidation capacity of the Arctic boundary layer (Sumner and Shepson, 1999). When O_3 is fully depleted, HCHO is the primary direct HO_x source via reaction with Br. This result explains the observation in Fig. 7, that on O_3-depleted days, the "Br Only" and "Br and Cl" simulations give essentially identical results for $[HO_2]$. Although these modeling results clearly indicate that Br-oxidation is the dominate HO_2 source during ODEs, the absolute value of the HO_2 production from this pathway during the ozone-depleted days should be regarded as an upper limit, since, as explained previously, the uncertainty in the BrO measurements is high during this time and it is possible that [Br] is somewhat overestimated. Indeed, this is likely the reason behind the high bias of the model HO_2 compared to measurements for 27 and 28 March (Fig. 2i).

A much more significant impact of chlorine chemistry on the oxidation capacity of the polar boundary layer (PBL) is the production of RO_2 through Reaction (R13) and analogous oxidation reactions with higher order hydrocarbons. RO_2 reaction with BrO can also lead to production of HOBr through Reaction (R17), which could enhance the heterogeneous production of Br through the bromine explosion mechanism.

$$\mathrm{BrO} + \mathrm{R{-}CH_2OO} \rightarrow \mathrm{HOBr} + \mathrm{R{-}CHOO} \qquad \text{(R17)}$$

However, the presence of chlorine chemistry also decreases the [BrO]/[Br] ratio through the BrO + ClO reaction, so Reaction (R17) may affect [HOBr] most under certain chemical conditions (e.g., lower [ClO]). The difference in simulated $[RO_2]$ (calculated as the sum of methyl through butyl forms) between simulations conducted with and without chlorine is shown in Fig. 9 (red trace vs. blue trace). As shown in Fig. 9, when Cl_2 is high, i.e. 25, 29, and 30 March, there is sometimes a large impact on RO_2

ACPD
14, 28685–28755, 2014

comparing the Br-only case with Base Model. Again, [Cl_2] is very low when ozone is depleted, so there is only a very small increase in modeled [RO_2] during ozone-depleted days due to chlorine chemistry. These results support the hypothesis that Cl can substantially increase the oxidation capacity of the Arctic troposphere when present at elevated mixing ratios. The levels of RO_2 that are present when Cl is not included in the model is primarily a result of both Br- and OH-oxidation chemistry; there is a significant increase in modeled RO_2 during ozone-depleted compared to background O_3 days due to the impact of Br-oxidation, in a similar fashion as discussed for HO_2 in Fig. 8. However, as RO_2 can significantly increase when Cl is present, is it apparent that Cl chemistry can be a major oxidant of VOCs in the Arctic. The impact of this increased RO_2 appears to be less significant as a BrO sink, however, as CH_3OO (the dominant RO_2 species) represents only a minor sink for BrO (Thompson et al., 2014), and BrO is likewise a minor sink for CH_3OO in comparison to HO_2 and NO (median sink contribution of BrO to CH3OO is 0.05 %).

Based on our analysis, it appears possible that the presence of chlorine can promote the production of reactive bromine species through two distinct mechanisms: (1) oxidation chemistry due to chlorine, which under certain chemical conditions can (e.g., high Cl_2, elevated NO_x) increase [HO_2] and/or [RO_2], thereby increasing the production of HOBr, and thus, the heterogeneous recycling of bromine, and (2) gas-phase HOCl can react with Br^- in the aqueous phase to produce BrCl, thus producing reactive bromine (though this pathway is not as significant for Br atom production as is Br_2). Conversely, the presence of both chloride and bromide ions in the aqueous phase can lead to a competition between the production of Br_2, BrCl, or Cl_2. In our model, large increases in gas-phase [Br] are produced when aerosol chloride is decreased by three orders of magnitude, but no difference in [Br] occurs when snowpack phase chloride is decreased by an equivalent amount. The snowpack is by far the primary source of both Br and Cl atom precursors in our model, as shown in Michalowski et al. (2000); however, the greater sensitivity to the aerosol chloride loading suggests that the aerosol could be a potentially important source of Cl atom precursors to the atmosphere. This

ACPD
14, 28685–28755, 2014

may likely be related to the aerosol pH. Laboratory and field studies would be required to test this hypothesis. It is clear that the interactions between bromine and chlorine are quite complex in that chlorine chemistry can produce reactive bromine sinks (when at elevated concentrations), but the presence of chlorine can also increase Br atom production under certain circumstances, thereby increasing the rate of ozone depletion in an indirect fashion.

4 The impact of iodine chemistry and bromine–iodine interactions

Several modeling studies have also investigated the potential impact of iodine on ozone depletion in the troposphere (e.g., Chameides and Davis, 1980; Davis et al., 1996; Sander et al., 1997; Calvert and Lindberg, 2004b; Saiz-Lopez et al., 2008), in each case concluding that it could be very important. Iodine is potentially one of the most important species in Arctic ozone chemistry, and yet there is very little observational information. To date, no conclusive measurements of IO in the High Arctic have been achieved, though recently our group has detected substantial concentrations of I_2 in the snowpack air in Barrow with CIMS, thus, there is evidence that iodine chemistry is present to some extent.

As discussed in Sect. 3.2, iodine chemistry can greatly enhance the rate of ozone depletion, both through the direct reaction of I with ozone (given that ozone is the primary I atom sink, Fig. 4) and through the indirect effect of increasing available Br atoms through the cross-reaction of IO and BrO. In a similar fashion, iodine chemistry also shifts the ClO_x partitioning, decreasing the mid-day [ClO]/[Cl] for 25 March from 359 in the base model (Br and Cl) to 328 when ~ 1 pptv IO is present due to the IO + ClO reaction and decreased $[O_3]$. The decreased [ClO]/[Cl] ratio could then impact the radical distribution through RO_2 production. The [IO]/[I] ratio is much lower than either the BrO_x or ClO_x ratio due to fast photolysis of IO and far fewer I atom sinks (Vogt, 1999). Under the conditions employed here on 25 March, the [IO]/[I] ratio is ~ 1.

ACPD
14, 28685–28755, 2014

Previous modeling studies have concluded that iodine chemistry can impact the partitioning of important atmospheric oxidants by decreasing the $[HO_2]/[OH]$ ratio through the formation of HOI and subsequent photolysis. Due to the approximately one order of magnitude faster rate constant for $IO + HO_2$ compared to $ClO + HO_2$, iodine has a greater impact on the $[HO_2]/[OH]$ ratio than does chlorine, and HO_2 can represent a primary IO sink during periods of low [IO] and [BrO] (Vogt, 1999). The $[HO_2]/[OH]$ ratio at mid-day on 25 March with no halogens present is 63. The presence of bromine alone decreases this ratio to 34, and inclusion of iodine further decreases this to 31; this is consistent with Saiz-Lopez et al. (2007b), who determined a ratio of 33 due to bromine–iodine chemistry in Antarctica.

The decrease in the ClO_x ratio affected by iodine could also impact the oxidizing capacity of the PBL. In fact, we see a slight increase in $[RO_2]$ when iodine is present at 1 pptv IO in the multiday model, with a greater increase during O_3-depleted days when iodine is included (green trace, Fig. 9). This effect is even greater for the 0.5 pptv I_2 scenario (orange trace). Because iodine atoms do not oxidize VOCs, the increased RO_2 is likely a result of the combined effects of a shift in the ClO_x ratio toward Cl, and a shift in the HO_x ratio toward OH, resulting in a decrease of RO_2 sinks. These impacts suggest an important indirect role for iodine in mediating the oxidation potential of the PBL.

We note, however, that the observed $[Cl_2]$ and $[Br_2]$ are lower during ozone-depleted days, than during non-ozone depleted days. This suggests a surface activation mechanism controlled by O_3, presumably in part through a snowpack halogen explosion mechanism, such as has been observed in laboratory studies by, e.g., Oum et al. (1998a, b) and the recent Pratt et al. (2013) study using natural Barrow snow. In our model, because the production mechanism of I_2 is undefined and we have no observations with which to compare, the I_2 flux is of the same magnitude each day, independent of $[O_3]$. Therefore, during the O_3 depleted days when $[Br_2]$ and $[Cl_2]$ are much reduced, iodine chemistry becomes dramatically more important in relative terms. However, laboratory studies have indicated that I_2 can be produced via O_3 ox-

ACPD
14, 28685–28755, 2014

idation of aqueous iodide (Garland and Curtis, 1981; Martino et al., 2009; Carpenter et al., 2013). If it were indeed the case that I_2 is also produced through an O_3-mediated activation mechanism, this would likely eliminate the large difference between depleted and non-depleted days that is seen here. More studies are required to determine the dominant mechanism and kinetics for the heterogeneous surface production of I_2.

As expected, the presence of halogen chemistry in our model increases the $[NO_2]/[NO]$ ratio, primarily through Reaction (R16), though Cl chemistry can further increase this ratio through the production of RO_2 (e.g., Reactions R13 – R14). However, though bromine increases the mid-day NO_x ratio from 0.66 to 1.70 for 25 March compared to a model run conducted with no halogens, the further addition of iodine only increases it to 1.93. The absolute concentrations of $[NO_2]$ and [NO] both decrease with the addition of halogens, but the $[NO_2]/[NO]$ ratio increases because XO reaction with NO is generally faster than reaction with NO_2. However, in the case of iodine, IO reaction with NO_2 is faster than its reaction with NO, and I atoms also react very efficiently with NO_2. Thus, chlorine has a greater effect on increasing the NO_x ratio than does iodine.

5 Conclusions

The goal of this work was to investigate the interactions and impacts of halogen chemistry on ozone depletion using a model that is constrained to observed, time-varying chemical conditions at the time of the event. With this approach, we have been able to dissect some of the important chemical pathways pertaining to ODEs, focusing on the interactions between the halogen radicals. From our analyses it is clear that the interactions between bromine, chlorine, and iodine are very complex and highly dependent on the concurrent conditions of relevant species, such as O_3, HO_x, NO_x, and the VOCs. As these species fluctuate, the partitioning of halogen species will also change, and so too will their impact on chemistry of the PBL. Thus, a full understanding of halogen

ACPD
14, 28685–28755, 2014

chemistry requires the careful measurement of all these species (including Cl_2, Br_2, HOBr and HOCl).

This work has demonstrated that bromine chemistry is clearly the dominant destruction pathway for ozone depletion episodes, but that chlorine and, especially, iodine, can contribute significantly to both the rate and timescale of ozone depletion. The new observations of high chlorine levels at Barrow potentially change the way we view ODEs. Often, observations of rapid decline in ozone at various locations have been attributed to transport because bromine chemistry alone was not enough to account for the ozone depletion rate (Hausmann and Platt, 1994; Tuckermann et al., 1997; Bottenheim et al., 2002). As we have shown, complete ozone depletions can occur on timescales of much less than a day, and at elevated chlorine levels, even as short as several hours. This result suggests that more of the ODEs that are observed could be the result of local scale chemistry, however, as noted previously, our calculated timescales for ozone depletion are based upon measurements conducted within the near surface layer and may not necessarily reflect the depletion timescale aloft. While chlorine is clearly not necessary to cause ozone depletion, it can significantly impact the rate of ozone depletion.

Moreover, the presence of elevated chlorine levels can impact important Arctic chemical budgets, including HO_x, NO_x and VOCs, with implications for the oxidative capacity of the PBL. More field measurements, including over the frozen Arctic Ocean, are necessary to evaluate the ubiquity of these elevated chlorine levels. In light of these new data, it is crucial that future Arctic modeling studies take into account the activity of chlorine.

In our model, we prescribed a Cl_2 mixing ratio that was varied from 16–400 pptv for 25 March in sensitivity studies to investigate the impact of elevated Cl_2. However, we also determined the Cl_2 fluxes that would be necessary to produce the desired gas-phase [Cl_2]. In our model, volumetric fluxes ranging from 5.5×10^5 molecules cm^{-3} s^{-1} to 1.45×10^6 molecules cm^{-3} s^{-1} were required. If we assume a boundary layer mixing height of 300 m, the corresponding surface fluxes would be 1.65×10^{10}–4.35×10^{10} molecules cm^{-2} s^{-1}. These numbers are consistent with those used by Piot and

ACPD
14, 28685–28755, 2014

von Glasow (2009). However, there are no Cl_2 measurements aloft of the surface in the Arctic. Utilizing the method of Guimbaud et al. (2002), the effective mixing height, Z^*, for Cl_2 at midday is only 2.15 m, making the calculated Cl_2 fluxes 1.2×10^8–3.1×10^8 molecules $cm^{-2}\,s^{-1}$. Therefore, field studies aimed at determining the magnitude of the surface flux of Cl_2 (and Br_2) are warranted. This disparity also points out the importance of measurements of the vertical profiles of molecular halogens above the snowpack/sea ice surface.

Finally, we find that iodine could be the most efficient halogen for depleting ozone on a per atom basis, given our assumed fluxes. We assume very low [IO] in our model ($\leq$ 1 pptv), below the detection limit of the DOAS instrumentation, and yet the resulting enhancements in ozone depletion are quite significant. Higher levels of iodine would certainly have a dramatic effect on ozone chemistry, as illustrated by our simulations incorporating 0.5 pptv I_2 (5–6 pptv IO). A possible mechanism for the production of I_2 in the polar regions is the activity of ice algae and phytoplankton that produce iodine-compounds, which are then wicked to the surface through brine channels (Mahajan et al., 2010). It has also been suggested that the primary productivity in Antarctic ice and waters may be higher than in the Arctic (Arrigo et al., 1997; Gosselin et al., 1997; Lizotte, 2001; Mahajan et al., 2010), possibly accounting for the difference in apparent iodine activity between the two poles. However, as the ice in the Arctic continues to thin, and as more multiyear ice has been replaced by seasonal sea ice (Nghiem et al., 2012), the algae and phytoplankton productivity in the Arctic has increased (Arrigo et al., 2008, 2012); this could lead to an increase in iodine emissions in the future, and thus to a greater occurrence of springtime ODEs. The further development of analytical methods capable of measuring the very low [IO] and [I_2] potentially present in the Arctic should be a high priority for the further advancement of this research.

Acknowledgements. The modeling analysis presented herein was funded by the National Science Foundation grant ARC-0732556. Partial support for CT during preparation of this manuscript was provided by the NSF Atmospheric and Geospace Sciences Postdoctoral Research Fellowship program. The authors wish to thank the organizers of the OASIS 2009

ACPD
14, 28685–28755, 2014

field campaign, the Barrow Arctic Science Consortium for logistics support, and all of the researchers who contributed to the campaign.

References

Adams, J. W., Holmes, N. S., and Crowley, J. N.: Uptake and reaction of HOBr on frozen and dry NaCl/NaBr surfaces between 253 and 233 K, Atmos. Chem. Phys., 2, 79–91, doi:10.5194/acp-2-79-2002, 2002.

Apel, E. C., Emmons, L. K., Karl, T., Flocke, F., Hills, A. J., Madronich, S., Lee-Taylor, J., Fried, A., Weibring, P., Walega, J., Richter, D., Tie, X., Mauldin, L., Campos, T., Weinheimer, A., Knapp, D., Sive, B., Kleinman, L., Springston, S., Zaveri, R., Ortega, J., Voss, P., Blake, D., Baker, A., Warneke, C., Welsh-Bon, D., de Gouw, J., Zheng, J., Zhang, R., Rudolph, J., Junkermann, W., and Riemer, D. D.: Chemical evolution of volatile organic compounds in the outflow of the Mexico City Metropolitan area, Atmos. Chem. Phys., 10, 2353–2375, doi:10.5194/acp-10-2353-2010, 2010.

Aranda, A., Le Bras, G., La Verdet, G., and Poulet, G.: The $BrO + CH_3O_2$ reaction: kinetics and role in the atmospheric ozone budget, Geophys. Res. Lett., 24, 2745–2748, 1997.

Ariya, P., Jobson, B., Sander, R., Niki, H., Harris, G., Hopper, J., and Anlauf, K.: Measurements of C2–C7 hydrocarbons during the Polar Sunrise Experiment 1994: further evidence for halogen chemistry in the troposphere, J. Geophys. Res., 103, 13169–13180, doi:10.1029/98JD00284, 1998.

Arrigo, K. R., Worthen, D. L., Lizotte, M. P., Dixon, P., and Dieckmann, G.: Primary production in Antarctic sea ice, Science, 276, 394–397, 1997.

Arrigo, K. R., van Dijken, G., and Pabi, S.: Impact of a shrinking Arctic ice cover on marine primary production, Geophys. Res. Lett, 35, L19603, doi:10.1029/2008GL035028, 2008.

Arrigo, K. R., Perovich, D. K., Pickart, R. S., Brown, Z. W., van Dijken, G. L., Lowry, K. E., Mills, M. M., Palmer, M. A., Balch, W. M., Bahr, F., Bates, N. R., Benitez-Nelson, C., Bowler, B., Brownlee, E., Ehn, J. K., Frey, K. E., Garley, R., Laney, S. R., Lubelczyk, L., Mathis, J., Matsuoka, A., Mitchell, B. G., Moore, G. W. K., Ortega-Retuerta, E., Pal, S., Polashenski, C. M., Reynolds, R. A., Schieber, B., Sosik, H. M., Stephens, M., and Swift, J. H.: Massive Phytoplankton Blooms Under Arctic Sea Ice, Science, 336, 1408, doi:10.1126/science.1215065, 2012.

Atkinson, R., Baulch, D. L., Cox, R. A., Crowley, J. N., Hampson, R. F., Hynes, R. G., Jenkin, M. E., Rossi, M. J., and Troe, J.: Evaluated kinetic and photochemical data for atmospheric chemistry: Volume I – gas phase reactions of O_x, HO_x, NO_x and SO_x species, Atmos. Chem. Phys., 4, 1461–1738, doi:10.5194/acp-4-1461-2004, 2004.

Barret, M., Domine, F., Houdier, S., Gallet, J. C., Weibring, P., Walega, J., Fried, A., and Richter, D.: Formaldehyde in the Alaskan Arctic snowpack: partitioning and physical processes involved in air-snow exchanges, J. Geophys. Res., 116, D00R03, doi:10.1029/2011JD016038, 2011.

Barrie, L., Bottenheim, J., Schnell, R., Crutzen, P., and Rasmussen, R.: Ozone destruction and photochemical reactions at polar sunrise in the lower Arctic atmosphere, Nature, 334, 138–141, 1988.

Barrie, L., Staebler, R., Toom, D., Georgi, B., Den Hartog, G., Landsberger, S., and Wu, D.: Arctic aerosol size-segregated chemical observations in relation to ozone depletion during Polar Sunrise Experiment 1992, J. Geophys. Res., 99, 25439–25451, 1994.

Beckwith, R. C., Wang, T. X., and Margerum, D. W.: Equilibrium and kinetics of bromine hydrolysis, Inorg. Chem., 35, 995–1000, 1996.

Beine, H. J., Honrath, R. E., Dominé, F., Simpson, W. R., and Fuentes, J. D.: NO_x during background and ozone depletion periods at Alert: fluxes above the snow surface, J. Geophys. Res., 107, 4584, doi:10.1029/2002JD002082, 2002.

Bottenheim, J. W., Fuentes, J. D., Tarasick, D. W., and Anlauf, K. G.: Ozone in the Arctic lower troposphere during winter and spring 2000 (ALERT2000), Atmos. Environ., 36, 2535–2544, 2002.

Bottenheim, J. W., Barrie, L. A., Atlas, E., Heidt, L. E., Niki, H., Rasmussen, R. A., and Shepson, P. B.: Depletion of lower tropospheric ozone during Arctic spring: the Polar Sunrise Experiment 1988, J. Geophys. Res., 95, 18555–18568, 1990.

Bottenheim, J. W. and Chan, E.: A trajectory study into the origin of spring time Arctic boundary layer ozone depletion, J. Geophys. Res., 111, D19301, doi:10.1029/2006JD007055, 2006.

Boudries, H. and Bottenheim, J.: Cl and Br atom concentrations during a surface boundary layer ozone depletion event in the Canadian high Arctic, Geophys. Res. Lett., 27, 517–520, 2000.

Calvert, J. and Lindberg, S.: A modeling study of the mechanism of the halogen-ozone-mercury homogeneous reactions in the troposphere during the polar spring, Atmos. Environ., 37, 4467–4481, 2003.

Calvert, J. G. and Lindberg, S. E.: The potential influence of iodine-containing compounds on the chemistry of the troposphere in the polar spring, II. Mercury depletion, Atmos. Environ., 38, 5105–5116, 2004a.
Calvert, J. G. and Lindberg, S. E.: Potential influence of iodine-containing compounds on the chemistry of the troposphere in the polar spring. I. Ozone depletion, Atmos. Environ., 38, 5087–5104, 2004b.
Carpenter, L., Sturges, W., Penkett, S., Liss, P., Alicke, B., Hebestreit, K., and Platt, U.: Short-lived alkyl iodides and bromides at Mace Head, Ireland: links to biogenic sources and halogen oxide production, J. Geophys. Res., 104, 1679–1689, 1999.
Carpenter, L. J., MacDonald, S. M., Shaw, M. D., Kumar, R., Saunders, R. W., Parthipan, R., Wilson, J., and Plane, J. M.: Atmospheric iodine levels influenced by sea surface emissions of inorganic iodine, Nat. Geosci., 6, 108–111, 2013.
Cavender, A. E., Biesenthal, T. A., Bottenheim, J. W., and Shepson, P. B.: Volatile organic compound ratios as probes of halogen atom chemistry in the Arctic, Atmos. Chem. Phys., 8, 1737–1750, doi:10.5194/acp-8-1737-2008, 2008.
Chameides, W. and Davis, D.: Iodine: its possible role in tropospheric photochemistry, J. Geophys. Res., 85, 7383–7398, 1980.
Cho, H., Shepson, P. B., Barrie, L. A., Cowin, J. P., and Zaveri, R.: NMR investigation of the quasi-brine layer in ice/brine mixtures, J. Phys. Chem.-US, 106, 11226–11232, 2002.
Clyne, M. and Cruse, H.: Atomic resonance fluorescence spectrometry for the rate constants of rapid bimolecular reactions, Part 2. Reactions Cl + BrCl, Cl + Br_2, Cl + ICl, Br + IBr, Br + ICl, J. Chem. Soc., 68, 1377–1387, 1972.
Davis, D., Crawford, J., Liu, S., McKeen, S., Bandy, A., Thornton, D., Rowland, F., and Blake, D.: Potential impact of iodine on tropospheric levels of ozone and other critical oxidants, J. Geophys. Res., 101, 2135–2147, 1996.
DeMore, W. B., Sander, S., Golden, D., Hampson, R., Kurylo, M., Howard, C., Ravishankara, A., Kolb, C., and Molina, M.: Chemical kinetics and photochemical data for use in stratospheric modeling, Jet Propulsion Lab., California Inst. of Tech., Pasadena, CA, 1997.
Donahue, N. M., Anderson, J. G., and Demerjian, K. L.: New rate constants for ten OH alkane reactions from 300 to 400 K: an assessment of accuracy, J. Phys. Chem.-US, 102, 3121–3126, 1998.
Dunlea, E. J. and Ravishankara, A.: Kinetic studies of the reactions of $O(^1D)$ with several atmospheric molecules, Phys. Chem. Chem. Phys., 6, 2152–2161, 2004.

ACPD
14, 28685–28755, 2014

Eberhard, J. and Howard, C. J.: Temperature-dependent kinetics studies of the reactions of $C_2H_5O_2$ and n-$C_3H_7O_2$ radicals with NO, Int. J. Chem. Kinet., 28, 731–740, 1996.
Eberhard, J., Villalta, P. W., and Howard, C. J.: Reaction of isopropyl peroxy radicals with NO over the temperature range 201–401 K, J. Phys. Chem.-US, 100, 993–997, 1996.
Fickert, S., Adams, J. W., and Crowley, J. N.: Activation of Br_2 and BrCl via uptake of HOBr onto aqueous salt solutions, J. Geophys. Res., 104, 23, 1999.
Fisher, J. A., Jacob, D. J., Wang, Q., Bahreini, R., Carouge, C. C., Cubison, M. J., Dibb, J. E., Diehl, T., Jimenez, J. L., and Leibensperger, E. M.: Sources, distribution, and acidity of sulfate-ammonium aerosol in the Arctic in winter-spring, Atmos. Environ., 45, 7301–7318, 2011.
Fried, A., Sewell, S., Henry, B., Wert, B. P., and Gilpin, T.: Tunable diode laser absorption spectrometer for ground-based measurements of formaldehyde, J. Geophys. Res., 102, 6253–6266, 1997.
Frieß, U., Deutschmann, T., Gilfedder, B. S., Weller, R., and Platt, U.: Iodine monoxide in the Antarctic snowpack, Atmos. Chem. Phys., 10, 2439–2456, doi:10.5194/acp-10-2439-2010, 2010.
Ganske, J., Berko, H., and Finlayson-Pitts, B.: Absorption Cross Sections for Gaseous $ClNO_2$ and Cl_2 at 298 K: potential Organic Oxidant Source in the Marine Troposphere, J. Geophys. Res., 97, 7651–7656, 1992.
Gao, S., Sjostedt, S., Sharma, S., Hall, S., Ullmann, K., and Abbatt, J.: PTR-MS observations of photo-enhanced VOC release from Arctic and mid-latitude snow, J. Geophys. Res., 117, D00R17, doi:10.1029/2011JD017152, 2012.
Garland, J. and Curtis, H.: Emission of iodine from the sea surface in the presence of ozone, J. Geophys. Res., 86, 3183–3186, 1981.
Gomez Martin, J. C., Spietz, P., and Burrows, J. P.: Spectroscopic studies of the I_2/O_3 photochemistry, Part 1: Determination of the absolute absorption cross sections of iodine oxides of atmospheric relevance, Journal of photochemistry and photobiology. A, Chemistry, 176, 15–38, 2005.
Gong, S., Walmsley, J., Barrie, L., and Hopper, J.: Mechanisms for surface ozone depletion and recovery during polar sunrise, Atmos. Environ., 31, 969–981, 1997.
Gosselin, M., Levasseur, M., Wheeler, P. A., Horner, R. A., and Booth, B. C.: New measurements of phytoplankton and ice algal production in the Arctic Ocean, Deep-Sea Res. Pt. II, 44, 1623–1644, 1997.

ACPD
14, 28685–28755, 2014

Grannas, A. M., Shepson, P. B., Guimbaud, C., Sumner, A. L., Albert, M., Simpson, W., Domine, F., Boudries, H., Bottenheim, J., and Beine, H. J.: A study of photochemical and physical processes affecting carbonyl compounds in the Arctic atmospheric boundary layer, Atmos. Environ., 36, 2733–2742, 2002.

Grannas, A. M., Jones, A. E., Dibb, J., Ammann, M., Anastasio, C., Beine, H. J., Bergin, M., Bottenheim, J., Boxe, C. S., Carver, G., Chen, G., Crawford, J. H., Dominé, F., Frey, M. M., Guzmán, M. I., Heard, D. E., Helmig, D., Hoffmann, M. R., Honrath, R. E., Huey, L. G., Hutterli, M., Jacobi, H. W., Klán, P., Lefer, B., McConnell, J., Plane, J., Sander, R., Savarino, J., Shepson, P. B., Simpson, W. R., Sodeau, J. R., von Glasow, R., Weller, R., Wolff, E. W., and Zhu, T.: An overview of snow photochemistry: evidence, mechanisms and impacts, Atmos. Chem. Phys., 7, 4329–4373, doi:10.5194/acp-7-4329-2007, 2007.

Guimbaud, C., Grannas, A. M., Shepson, P. B., Fuentes, J. D., Boudries, H., Bottenheim, J. W., Dominé, F., Houdier, S., Perrier, S., and Biesenthal, T. B.: Snowpack processing of acetaldehyde and acetone in the Arctic atmospheric boundary layer, Atmos. Environ., 36, 2743–2752, 2002.

Halfacre, J. W., Knepp, T. N., Shepson, P. B., Thompson, C. R., Pratt, K. A., Li, B., Peterson, P. K., Walsh, S. J., Simpson, W. R., Matrai, P. A., Bottenheim, J. W., Netcheva, S., Perovich, D. K., and Richter, A.: Temporal and spatial characteristics of ozone depletion events from measurements in the Arctic, Atmos. Chem. Phys., 14, 4875–4894, doi:10.5194/acp-14-4875-2014, 2014.

Hansen, J. C., Li, Y., Li, Z., and Francisco, J. S.: On the mechanism of the BrO + HBr reaction, Chem. Phys. Lett., 314, 341–346, 1999.

Harris, S. J. and Kerr, J. A.: Relative rate measurements of some reactions of hydroxyl radicals with alkanes studied under atmospheric conditions, Int. J. Chem. Kinet., 20, 939–955, 1988.

Hausmann, M. and Platt, U.: Spectroscopic measurement of bromine oxide and ozone in the high Arctic during Polar Sunrise Experiment 1992, J. Geophys. Res., 99, 25399–25413, 1994.

Helmig, D., Ganzeveld, L., Butler, T., and Oltmans, S. J.: The role of ozone atmosphere-snow gas exchange on polar, boundary-layer tropospheric ozone – a review and sensitivity analysis, Atmos. Chem. Phys., 7, 15–30, doi:10.5194/acp-7-15-2007, 2007.

Helmig, D., Boylan, P., Johnson, B., Oltmans, S., Fairall, C., Staebler, R., Weinheimer, A., Orlando, J., Knapp, D. J., Montzka, D. D., Flocke, F., Frieß, U., Sihler, H., and Shepson, P. B.:

Ozone dynamics and snow-atmosphere exchanges during ozone depletion events at Barrow, Alaska, J. Geophys. Res., 117, D20303, doi:10.1029/2012JD017531, 2012.
Hönninger, G.: Halogen Oxide Studies in the Boundary Layer by Multi Axis Differential Optical Absorption Spectroscopy and Active Longpath-DOAS, Ph. D., University of Heidelberg, 2002.
Honrath, R., Peterson, M., Guo, S., Dibb, J., Shepson, P., and Campbell, B.: Evidence of NOx production within or upon ice particles in the Greenland snowpack, Geophys. Res. Lett, 26, 695–698, 1999.
Hooshiyar, P. A. and Niki, H.: Rate constants for the gas phase reactions of Cl atoms with C2–C8 alkanes at $T = 296 \pm 2$ K, Int. J. Chem. Kinet., 27, 1197–1206, 1995.
Huff, A. K. and Abbatt, J. P. D.: Kinetics and product yields in the heterogeneous reactions of HOBr with ice surfaces containing NaBr and NaCl, J. Phys. Chem. A, 106, 5279–5287, 2002.
Impey, G., Shepson, P., Hastie, D., Barrie, L., and Anlauf, K.: Measurements of photolyzable chlorine and bromine during the Polar Sunrise Experiment 1995, J. Geophys. Res., 102, 16005–16010, 1997.
Jacob, D. J.: Heterogeneous chemistry and tropospheric ozone, Atmos. Environ., 34, 2131–2159, 2000.
Jacobi, H. W., Kaleschke, L., Richter, A., Rozanov, A., and Burrows, J. P.: Observation of a fast ozone loss in the marginal ice zone of the Arctic Ocean, J. Geophys. Res.-Atmos., 111, D15309 doi:10.1029/2005JD006715, 2006.
Jobson, B., Niki, H., Yokouchi, Y., Bottenheim, J., Hopper, F., and Leaitch, R.: Measurements of C2–C6 hydrocarbons during the Polar Sunrise 1992 Experiment: evidence for Cl atom and Br atom chemistry, J. Geophys. Res., 99, 25355–25368, 1994.
Jones, C. E., Hornsby, K. E., Sommariva, R., Dunk, R. M., von Glasow, R., McFiggans, G., and Carpenter, L. J.: Quantifying the contribution of marine organic gases to atmospheric iodine, Geophys. Res. Lett., 37, L18804, doi:10.1029/2005JD006715, 2010.
Kamboures, M. A., Hansen, J. C., and Francisco, J. S.: A study of the kinetics and mechanisms involved in the atmospheric degradation of bromoform by atomic chlorine, Chem. Phys. Lett., 353, 335–344, 2002.
Keil, A. and Shepson, P.: Chlorine and bromine atom ratios in the springtime Arctic troposphere as determined from measurements of halogenated volatile organic compounds, J. Geophys. Res., 111, D17303, doi:10.1029/2006JD007119, 2006.

ACPD
14, 28685–28755, 2014

King, M. D. and Simpson, W. R.: Extinction of UV radiation in Arctic snow at Alert, Canada (82° N), J. Geophys. Res., 106, 499–412, 2001.

Kirchner, F. and Stockwell, W. R.: Effect of peroxy radical reactions on the predicted concentrations of ozone, nitrogenous compounds, and radicals, J. Geophys. Res., 101, 21007–21022, 1996.

Knepp, T. N., Bottenheim, J., Carlsen, M., Carlson, D., Donohoue, D., Friederich, G., Matrai, P. A., Netcheva, S., Perovich, D. K., Santini, R., Shepson, P. B., Simpson, W., Valentic, T., Williams, C., and Wyss, P. J.: Development of an autonomous sea ice tethered buoy for the study of ocean-atmosphere-sea ice-snow pack interactions: the O-buoy, Atmos. Meas. Tech., 3, 249–261, doi:10.5194/amt-3-249-2010, 2010.

Krnavek, L., Simpson, W. R., Carlson, D., Domine, F., Douglas, T. A., and Sturm, M.: The chemical composition of surface snow in the Arctic: examining marine, terrestrial, and atmospheric influences, Atmos. Environ.,50, 349–359, 2012.

Kukui, A., Kirchner, U., Benter, T., and Schindler, R.: A gaskinetic investigation of HOBr reactions with Cl (2P), O (3P) and OH (2II). The reaction of BrCl with OH (2II), Berichte der Bunsengesellschaft für physikalische Chemie, 100, 455–461, 1996.

Lancaster, D. G., Fried, A., Wert, B., Henry, B., and Tittel, F. K.: Difference-frequency-based tunable absorption spectrometer for detection of atmospheric formaldehyde, Appl. Optics, 39, 24, 4436–4443, 2000.

Le Bras, G. and Platt, U.: A possible mechanism for combined chlorine and bromine catalyzed destruction of tropospheric ozone in the Arctic, Geophys. Res. Lett., 22, 599–602, 1995.

Lehrer, E., Hönninger, G., and Platt, U.: A one dimensional model study of the mechanism of halogen liberation and vertical transport in the polar troposphere, Atmos. Chem. Phys., 4, 2427–2440, doi:10.5194/acp-4-2427-2004, 2004.

Li, S.-M., and Winchester, J. W.: Resolution of ionic components of late winter Arctic aerosols, Atmos. Environ., 23, 2387–2399, 1989.

Liao, J., Sihler, H., Huey, L. G., Neumann, J. A., Tanner, D. J., Friess, U., Platt, U., Flocke, F. M., Orlando, J. J., Shepson, P. B., Beine, H. J., Weinheimer, A. J., Sjostedt, S. J., Nowak, J. B., Knapp, D. J., Staebler, R. M., Zheng, W., Sander, R., Hall, S. R., and Ullmann, K.: A comparison of Arctic BrO measurements by chemical ionization mass spectrometry and long-path differential optical absorption spectroscopy, J. Geophys. Res., 116, D00R02, doi:10.1029/2010JD014788, 2011.

Liao, J., Huey, L., Tanner, D., Flocke, F., Orlando, J., Neuman, J., Nowak, J., Weinheimer, A., Hall, S., Smith, J., Fried, A., Staebler, R., Wang, Y., Koo, J.-H., Cantrell, C., Weibring, P., Walega, J., Knapp, D., Shepson, P., and Stephens, C.: Observations of inorganic bromine (HOBr, BrO, and Br_2) speciation at Barrow, Alaska, in spring 2009, J. Geophys. Res., 117, D00R16, doi:10.1029/2011JD016641, 2012.

Liao, J., Huey, L. G., Liu, Z., Tanner, D. J., Cantrell, C. A., Orlando, J. J., Flocke, F. M., Shepson, P. B., Weinheimer, A. J., Hall, S. R., Ullmann, K., Beine, H. J., Wang, Y., Ingall, E. D., Stephens, C. R., Hornbrook, R. S., Apel, E. C., Riemer, D., Fried, A., Mauldin III, R. L., Smith, J. N., Staebler, R. M., Neuman, J. A., and Nowak, J. B.: High levels of molecular chlorine in the Arctic atmosphere, Nat. Geosci., 7, 91–94, doi:10.1038/ngeo2046, 2014.

Lightfoot, P., Cox, R., Crowley, J., Destriau, M., Hayman, G., Jenkin, M., Moortgat, G., and Zabel, F.: Organic peroxy radicals: kinetics, spectroscopy and tropospheric chemistry, Atmos. Environ., 26, 1805–1961, 1992.

Lizotte, M. P.: The contributions of sea ice algae to Antarctic marine primary production, Am. Zool., 41, 57–73, 2001.

Lurmann, F. W., Lloyd, A. C., and Atkinson, R.: A chemical mechanism for use in long-range transport/acid deposition computer modeling, J. Geophys. Res., 91, 10905–10936, 1986.

Madronich, S. and Flocke, S.: The role of solar radiation in atmospheric chemistry, in: Handbook of Environmental Chemistry, 1–26, 1999.

Mahajan, A., Shaw, M., Oetjen, H., Hornsby, K., Carpenter, L., Kaleschke, L., Tian-Kunze, X., Lee, J., Moller, S., and Edwards, P.: Evidence of reactive iodine chemistry in the Arctic boundary layer, J. Geophys. Res., 115, D20303, doi:10.1029/2009JD013665, 2010.

Mallard, W. G., Westley, F., Herron, J. T., Hampson, R. F., and Frizzel, D. H.: NIST Chemical Kinetics Database: Version 5.0, National Institute of Standards and Technology, Gaithersburg, MD, 1993.

Martinez, M., Arnold, T., and Perner, D.: The role of bromine and chlorine chemistry for arctic ozone depletion events in Ny-Ålesund and comparison with model calculations, Ann. Geophys., 17, 941–956, doi:10.1007/s00585-999-0941-4, 1999.

Martino, M., Mills, G. P., Woeltjen, J., and Liss, P. S.: A new source of volatile organoiodine compounds in surface seawater, Geophys. Res. Lett., 36, L01609, doi:10.1029/2008GL036334, 2009.

ACPD
14, 28685–28755, 2014

McFiggans, G., Plane, J. M. C., Allan, B. J., Carpenter, L. J., Coe, H., and O'Dowd, C.: A modeling study of iodine chemistry in the marine boundary layer, J. Geophys. Res., 105, 14371–14385, doi:10.1029/1999JD901187, 2000.

McFiggans, G., Cox, R. A., Mössinger, J. C., Allan, B. J., and Plane, J. M. C.: Active chlorine release from marine aerosols: roles for reactive iodine and nitrogen species, J. Geophys. Res., 107, 4271, doi:10.1029/2001JD000383, 2002.

Michalowski, B. A., Francisco, J. S., Li, S. M., Barrie, L. A., Bottenheim, J. W., and Shepson, P. B.: A computer model study of multiphase chemistry in the Arctic boundary layer during polar sunrise, J. Geophys. Res., 105, 15131–15145, doi:10.1029/2000JD900004, 2000.

Nghiem, S. V., Rigor, I. G., Richter, A., Burrows, J. P., Shepson, P. B., Bottenheim, J. W., Barber, D. G., Steffen, A., Latonas, J. R., Wang, F., Stern, G., Clemente-Colón, P., Martin, S., Hall, D. K., Kaleschke, L, Tackett, P., Neumann, G., and Asplin, M.: Field and satellite observations of the formation and distribution of Arctic atmospheric bromine above a rejuvenated sea ice cover, J. Geophys. Res., 117, D00S05, doi:10.1029/2011JD016268, 2012.

Nicovich, J. and Wine, P.: Kinetics of the reactions of O (3P) and Cl (2P) with HBr and Br_2, Int. J. Chem. Kinet., 22, 379–397, 1990.

Oltmans, S. J. and Komhyr, W. D.: Surface ozone distributions and variations from 1973–1984 measurements at the NOAA geophysical monitoring for climatic change baseline observatories, J. Geophys. Res., 91, 5229–5236, 1986.

Oltmans, S. J., Johnson, B. J., and Harris, J. M.: Springtime boundary layer ozone depletion at Barrow, Alaska: meteorological influence, year-to-year variation, and long-term change, J. Geophys. Res., 117, D00R18, doi:10.1029/2011jd016889, 2012.

Orlando, J. J. and Tyndall, G. S.: Rate Coefficients for the Thermal Decomposition of $BrONO_2$ and the heat of formation of $BrONO_2$, J. Phys. Chem.-US, 100, 19398–19405, 1997.

Oum, K., Lakin, M., DeHaan, D., Brauers, T., and Finlayson-Pitts, B.: Formation of molecular chlorine from the photolysis of ozone and aqueous sea-salt particles, Science, 279, 74, 1998a.

Oum, K., Lakin, M., and Finlayson-Pitts, B.: Bromine activation in the troposphere by the dark reaction of O_3 with seawater ice, Geophys. Res. Lett., 25, 3923–3926, 1998b.

Piot, M. and von Glasow, R.: The potential importance of frost flowers, recycling on snow, and open leads for ozone depletion events, Atmos. Chem. Phys., 8, 2437–2467, doi:10.5194/acp-8-2437-2008, 2008.

ACPD
14, 28685–28755, 2014

Piot, M. and von Glasow, R.: Modelling the multiphase near-surface chemistry related to ozone depletions in polar spring, J. Atmos. Chem., 64, 77–105, 2009.
Platt, U. and Janssen, C.: Observation and role of the free radicals NO_3, ClO, BrO and IO in the troposphere, Faraday Discuss., 100, 175–198, 1995.
Platt, U. and Hönninger, G.: The role of halogen species in the troposphere, Chemosphere, 52, 325–338, 2003.
Pöhler, D., Vogel, L., Frieß, U., and Platt, U.: Observation of halogen species in the Amundsen Gulf, Arctic, by active long-path differential optical absorption spectroscopy, P. Natl. Acad. Sci. USA, 107, 6582–6587, doi:10.1073/pnas.0912231107, 2010.
Pratt, K. A., Custard, K. D., Shepson, P. B., Douglas, T. A., Pöhler, D., General, S., Zielcke, J., Simpson, W. R., Platt, U., and Tanner, D. J.: Photochemical production of molecular bromine in Arctic surface snowpacks, Nat. Geosci., 6, 351–356, 2013.
Ridley, B., Grahek, F., and Walega, J.: A small high-sensitivity, medium-response ozone detector suitable for measurements from light aircraft, J. Atmos. Ocean. Tech., 9, 142–148, 1992.
Roberts, J. M., Osthoff, H. D., Brown, S. S., and Ravishankara, A.: N_2O_5 oxidizes chloride to Cl2 in acidic atmospheric aerosol, Science, 321, 1059–1059, 2008.
Rudolph, J., Fu, B., Thompson, A., Anlauf, K., and Bottenheim, J.: Halogen atom concentrations in the Arctic troposphere derived from hydrocarbon measurements: impact on the budget of formaldehyde, Geophys. Res. Lett., 26, 2941–2944, 1999.
Russo, R. S., Zhou, Y., White, M. L., Mao, H., Talbot, R., and Sive, B. C.: Multi-year (2004–2008) record of nonmethane hydrocarbons and halocarbons in New England: seasonal variations and regional sources, Atmos. Chem. Phys., 10, 4909–4929, doi:10.5194/acp-10-4909-2010, 2010.
Ryerson, T. B., Williams, E. J., and Fehsenfeld, F. C.: An efficient photolysis system for fast-response NO_2 measurements, J. Geophys. Res., 105, 26447–26461, 2000.
Saiz-Lopez, A. and Plane, J. M. C.: Novel iodine chemistry in the marine boundary layer, Geophys. Res. Lett., 31, L04112, doi:10.1029/2003GL019215, 2004.
Saiz-Lopez, A., Chance, K., Liu, X., and Kurosu, T. P.: First observations of iodine oxide from space, 2007a.
Saiz-Lopez, A., Mahajan, A. S., Salmon, R. A., Bauguitte, S. J. B., Jones, A. E., Roscoe, H. K., and Plane, J.: Boundary layer halogens in coastal Antarctica, Science, 317, 348–351, doi:10.1126/science.1141408, 2007b.

ACPD
14, 28685–28755, 2014

Saiz-Lopez, A., Plane, J. M. C., Mahajan, A. S., Anderson, P. S., Bauguitte, S. J.-B., Jones, A. E., Roscoe, H. K., Salmon, R. A., Bloss, W. J., Lee, J. D., and Heard, D. E.: On the vertical distribution of boundary layer halogens over coastal Antarctica: implications for O_3, HO_x, NO_x and the Hg lifetime, Atmos. Chem. Phys., 8, 887–900, doi:10.5194/acp-8-887-2008, 2008.

Saiz-Lopez, A., Plane, J. M. C., Baker, A. R., Carpenter, L. J., von Glasow, R., Gomez Martin, J. C., McFiggans, G., and Saunders, R. W.: Atmospheric Chemistry of Iodine, Chem. Rev., 112, 1773–1804, doi:10.1021/cr200029u, 2011.

Sander, R. and Crutzen, P. J.: Model study indicating halogen activation and ozone destruction in polluted air masses transported to the sea, J. Geophys. Res., 101, 9121–9138, 1996.

Sander, R., Vogt, R., Harris, G. W., and Crutzen, P. J.: Modelling the chemistry of ozone, halogen compounds, and hydrocarbons in the arctic troposphere during spring, Tellus B, 49, 522–532, 1997.

Sander, S. P., Golden, D., Kurylo, M., Moortgat, G., Wine, P., Ravishankara, A., Kolb, C., Molina, M., Finlayson-Pitts, B., and Huie, R.: Chemical kinetics and photochemical data for use in atmospheric studies, evaluation number 15, 2006.

Saunders, R. W. and Plane, J. M. C.: Formation pathways and composition of iodine oxide ultra-fine particles, Environ. Chem., 2, 299–303, 2006.

Schönhardt, A., Richter, A., Wittrock, F., Kirk, H., Oetjen, H., Roscoe, H. K., and Burrows, J. P.: Observations of iodine monoxide columns from satellite, Atmos. Chem. Phys., 8, 637–653, doi:10.5194/acp-8-637-2008, 2008.

Schweitzer, F., Mirabel, P., and George, C.: Multiphase chemistry of N_2O_5, $ClNO_2$, and $BrNO_2$, J. Phys. Chem.-US, 102, 3942–3952, 1998.

Shepson, P. B., Sirju, A.-P., Hopper, J. F., Barrie, L. A., Young, V., Niki, H., and Dryfhout, H.: Sources and sinks of carbonyl compounds in the Arctic Ocean boundary layer: Polar Ice Floe Experiment, J. Geophys. Res., 101, 21081–21089, doi:10.1029/96JD02032, 1996.

Simpson, W. R., von Glasow, R., Riedel, K., Anderson, P., Ariya, P., Bottenheim, J., Burrows, J., Carpenter, L. J., Frieß, U., Goodsite, M. E., Heard, D., Hutterli, M., Jacobi, H.-W., Kaleschke, L., Neff, B., Plane, J., Platt, U., Richter, A., Roscoe, H., Sander, R., Shepson, P., Sodeau, J., Steffen, A., Wagner, T., and Wolff, E.: Halogens and their role in polar boundary-layer ozone depletion, Atmos. Chem. Phys., 7, 4375–4418, doi:10.5194/acp-7-4375-2007, 2007.

Sirois, A. and Barrie, L. A.: Arctic lower tropospheric aerosol trends and composition at Alert, Canada: 1980–1995, J. Geophys. Res., 104, 11599–11618, 1999.
Sommariva, R., Bloss, W., and von Glasow, R.: Uncertainties in gas-phase atmospheric iodine chemistry, Atmos. Environ., 57, 219–232, 2012.
Stephens, C. R., Shepson, P. B., Steffen, A., Bottenheim, J. W., Liao, J., Huey, L. G., Apel, E., Weinheimer, A., Hall, S. R., and Cantrell, C.: The relative importance of chlorine and bromine radicals in the oxidation of atmospheric mercury at Barrow, Alaska, J. Geophys. Res., 117, D00R11, doi:10.1029/96JD02032, 2012.
Sturges, W. and Barrie, L.: Chlorine, bromine and iodine in Arctic aerosols, Atmos. Environ., 22, 1179–1194, 1988.
Sumner, A., Shepson, P., Grannas, A., Bottenheim, J., Anlauf, K., Worthy, D., Schroeder, W., Steffen, A., Domine, F., and Perrier, S.: Atmospheric chemistry of formaldehyde in the Arctic troposphere at Polar Sunrise, and the influence of the snowpack, Atmos. Environ., 36, 2553–2562, 2002.
Sumner, A. L. and Shepson, P. B.: Snowpack production of formaldehyde and its effect on the Arctic troposphere, Nature, 398, 230–233, 1999.
Tackett, P., Cavender, A., Keil, A., Shepson, P., Bottenheim, J., Morin, S., Deary, J., Steffen, A., and Doerge, C.: A Study of the vertical scale of halogen chemistry in the Arctic troposphere during polar sunrise at Barrow, AK, J. Geophys. Res., 112, D07306, doi:10.1029/2006JD007785, 2007.
Tang, T. and McConnell, J.: Autocatalytic release of bromine from Arctic snow pack during polar sunrise, Geophys. Res. Lett., 23, 2633–2636, 1996.
Thomas, J. L., Stutz, J., Lefer, B., Huey, L. G., Toyota, K., Dibb, J. E., and von Glasow, R.: Modeling chemistry in and above snow at Summit, Greenland – Part 1: Model description and results, Atmos. Chem. Phys., 11, 4899–4914, doi:10.5194/acp-11-4899-2011, 2011.
Thomas, J. L., Dibb, J. E., Huey, L. G., Liao, J., Tanner, D., Lefer, B., von Glasow, R., and Stutz, J.: Modeling chemistry in and above snow at Summit, Greenland – Part 2: Impact of snowpack chemistry on the oxidation capacity of the boundary layer, Atmos. Chem. Phys., 12, 6537–6554, doi:10.5194/acp-12-6537-2012, 2012.
Troy, R. C., Kelley, M. D., Nagy, J. C., and Margerum, D. W.: Non-metal redox kinetics: iodine monobromide reaction with iodide ion and the hydrolysis of IBr, Inorg. Chem., 30, 4838–4845, 1991.

ACPD
14, 28685–28755, 2014

Tsalkani, N., Mellouki, A., Poulet, G., Toupance, G., and Bras, G.: Rate constant measurement for the reactions of OH and Cl with peroxyacetyl nitrate at 298 K, J. Atmos. Chem., 7, 409–419, 1988.

Tuckermann, M., Ackermann, R., Gölz, C., Lorenzen-Schmidt, H., Senne, T., Stutz, J., Trost, B., Unold, W., and Platt, U.: DOAS-observation of halogen radical-catalysed arctic boundary layer ozone destruction during the ARCTOC-campaigns 1995 and 1996 in Ny-Ålesund, Spitsbergen, Tellus B, 49, 533–555, 1997.

Tyndall, G., Orlando, J., Wallington, T., Dill, M., and Kaiser, E.: Kinetics and mechanisms of the reactions of chlorine atoms with ethane, propane, and n-butane, Int. J. Chem. Kinet., 29, 43–55, 1997.

Vakhtin, A. B., Murphy, J. E., and Leone, S. R.: Low-temperature kinetics of reactions of OH radical with ethene, propene, and 1-butene, J. Phys. Chem.-US, 107, 10055–10062, 2003.

Villena, G., Wiesen, P., Cantrell, C. A., Flocke, F., Fried, A., Hall, S. R., Hornbrook, R. S., Knapp, D., Kosciuch, E., Mauldin III, R. L., McGrath, J. A., Montzka, D., Richter, D., Ullmann, K., Walega, J., Weibring, P., Weinheimer, A., Staebler, R. M., Liao, J., Huey, L. G., and Kleffmann, J.: Nitrous acid (HONO) during polar spring in Barrow, Alaska: a net source of OH radicals?, J. Geophys. Res., 116, D00R07, doi:10.1029/2011JD016643, 2011.

Vogt, R., Crutzen, P. J., and Sander, R.: A mechanism for halogen release from sea-salt, Nature, 383, 26, 1996.

Vogt, R.: Iodine compounds in the atmosphere, reactive halogen compounds in the atmosphere, 113–128, 1999.

Wallington, T. J., Skewes, L. M., Siegl, W. O., Wu, C. H., and Japar, S. M.: Gas phase reaction of Cl atoms with a series of oxygenated organic species at 295 K, Int. J. Chem. Kinet., 20, 867–875, 1988.

Wallington, T. J., Skewes, L. M., Siegl, W. O., and Japar, S. M.: A relative rate study of the reaction of bromine atoms with a variety of organic compounds at 295 K, Int. J. Chem. Kinet., 21, 1069–1076, 1989.

Wang, T. X. and Margerum, D. W.: Kinetics of reversible chlorine hydrolysis: temperature dependence and general-acid/base-assisted mechanisms, Inorg. Chem., 33, 1050–1055, 1994.

Wang, T. X., Kelley, M. D., Cooper, J. N., Beckwith, R. C., and Margerum, D. W.: Equilibrium, kinetic, and UV-spectral characteristics of aqueous bromine chloride, bromine, and chlorine species, Inorg. Chem., 33, 5872–5878, 1994.

ACPD
14, 28685–28755, 2014

Wang, Y. L., Nagy, J. C., and Margerum, D. W.: Kinetics of hydrolysis of iodine monochloride measured by the pulsed-accelerated-flow method, J. Am. Chem. Soc., 111, 7838–7844, 1989.

Wine, P., Wells, J., and Nicovich, J.: Kinetics of the reactions of atomic fluorine (2P) and atomic chlorine (2P) with nitric acid, J. Phys. Chem.-US, 92, 2223–2228, 1988.

Zhou, X., Beinel, H. J., Honrath, R. E., Fuentes, J. D., Simpson, W., Shepson, P. B., and Bottenheim, J. W.: Snowpack Photochemical Production of HONO: a major source of OH in the Arctic boundary layer in springtime, Geophys. Res. Lett., 28, 4087–4090, 2001.

ACPD
14, 28685–28755, 2014

Table 1. Gas-phase chemical reactions used in the model. All rate constants are calculated for a temperature of 248 K unless otherwise noted and are expressed in units of $cm^3\ molecule^{-1}\ s^{-1}$.

Reaction	Rate Constant	Reference
$O(^1D) + M \rightarrow O(^3P)$	7.22×10^{-11}	Dunlea et al. (2002)
$O(^3P) + O_2 \rightarrow O_3$	2.12×10^{-14}	Atkinson et al. (2004)
$O(^1D) + H_2O \rightarrow 2OH$	2.2×10^{-10}	Atkinson et al. (2004)
$OH + O_3 \rightarrow HO_2$	3.84×10^{-14}	Atkinson et al. (2004)
$OH + HO_2 \rightarrow H_2O$	1.34×10^{-10}	Atkinson et al. (2004)
$OH + H_2O_2 \rightarrow HO_2 + H_2O$	1.52×10^{-12}	Atkinson et al. (2004)
$OH + O(^3P) \rightarrow O_2$	3.74×10^{-11}	Atkinson et al. (2004)
$OH + OH \rightarrow H_2O + O(^3P)$	1.74×10^{-12}	Atkinson et al. (2004)
$OH + OH \rightarrow H_2O_2$	1.86×10^{-11}	Atkinson et al. (2004)
$OH + NO_3 \rightarrow HO_2 + NO_2$	2.0×10^{-11}	Atkinson et al. (2004)
$HO_2 + NO_3 \rightarrow HNO_3$	4.0×10^{-12}	Atkinson et al. (2004)
$HO_2 + O_3 \rightarrow OH + 2O_2$	1.39×10^{-15}	Atkinson et al. (2004)
$HO_2 + HO_2 \rightarrow H_2O_2 + O_2$	2.58×10^{-12}	Atkinson et al. (2004)
$NO + OH \rightarrow HONO$	3.49×10^{-11}	Atkinson et al. (2004)
$NO + HO_2 \rightarrow NO_2 + OH$	9.59×10^{-12}	Atkinson et al. (2004)
$NO + O_3 \rightarrow NO_2$	7.09×10^{-15}	Sander et al. (2006)
$NO + NO_3 \rightarrow NO_2 + NO_2$	2.98×10^{-11}	Sander et al. (2006)
$NO_2 + OH \rightarrow HNO_3$	1.2×10^{-10}	Atkinson et al. (2004)
$NO_2 + HO_2 \leftrightarrow HNO_4$	$f: 8.6 \times 10^{-12}$ $r: 1.32 \times 10^{-4}$	Atkinson et al. (2004)
$NO_2 + O_3 \rightarrow NO_3$	6.15×10^{-18}	Sander et al. (2006)
$NO_2 + NO_3 \leftrightarrow N_2O_5$	$f: 1.83 \times 10^{-12}$ $r: 3.76 \times 10^{-5}$	Atkinson et al. (2004)
$NO_2 + CH_3COOO \leftrightarrow PAN$	$f: 1.4 \times 10^{-11}$ $r: 3.1 \times 10^{-8}$	Atkinson et al. (2004)
$NO_3 + NO_3 \rightarrow NO_2 + NO_2$	4.36×10^{-17}	Sander et al. (2006)
$N_2O_5 + H_2O \rightarrow HNO_3 + HNO_3$	2.6×10^{-22}	Atkinson et al. (2004)
$HONO + OH \rightarrow NO_2 + H_2O$	3.74×10^{-12}	Sander et al. (2006)
$HNO_3 + OH \rightarrow NO_3 + H_2O$	1.5×10^{-13}	Atkinson et al. (2004)
$HNO_4 + OH \rightarrow NO_2 + H_2O$	6.2×10^{-12}	Atkinson et al. (2004)
$CO + OH \rightarrow HO_2 + CO_2$	2.4×10^{-13}	Atkinson et al. (2004)
$CH_4 + OH \rightarrow CH_3OO + H_2O$	1.87×10^{-15}	Sander et al. (2006)
$C_2H_2 + OH \rightarrow C_2H_2OH$	7.8×10^{-13}	Atkinson et al. (2004)
$C_2H_6 + OH \rightarrow C_2H_5OO$	1.18×10^{-13}	Lurmann et al. (1986)
$C_2H_4 + OH \rightarrow C_2H_4OH$	1.02×10^{-11}	Vakhtin et al. (2003)
$C_3H_8 + OH \rightarrow nC_3H_7O_2$	1.56×10^{-13}	Harris and Kerr (1988)
$C_3H_8 + OH \rightarrow iC_3H_7O_2$	6.64×10^{-13}	Harris and Kerr (1988)

ACPD
14, 28685–28755, 2014

Table 1. Continued.

Reaction	Rate Constant	Reference
$C_3H_6 + OH \rightarrow C_3H_6OH$	3.63×10^{-11}	Atkinson et al. (2004)
$C_3H_6O + OH \rightarrow$ Products	2.51×10^{-11}	Atkinson et al. (2004)
$nC_3H_7O_2 + NO \rightarrow NO_2 + C_3H_6O + HO_2$	5.4×10^{-11}	Eberhard et al. (1996)
$iC_3H_7O_2 + NO \rightarrow NO_2 + CH_3COCH_3 + HO_2$	1.2×10^{-11}	Eberhard and Howard (1996)
$nC_4H_{10} + OH \rightarrow nC_4H_9OO$	1.64×10^{-12}	Donahue et al. (1998)
$iC_4H_{10} + OH \rightarrow CH_3COCH_3 + CH_3OO$	1.65×10^{-12}	Donahue et al. (1998)
$nC_4H_9OO + NO \rightarrow$ n-Butanal $+ NO_2 + HO_2$	5.4×10^{-11}	Michalowski et al. (2000)
$nC_4H_9OO + CH_3OO \rightarrow$ n-Butanal $+ HCHO + HO_2 + HO_2$	6.7×10^{-13}	Michalowski et al. (2000)
$nC_4H_9OO + CH_3OO \rightarrow$ n-Butanal $+ CH_3OH$	2.3×10^{-13}	Michalowski et al. (2000)
$nC_4H_9OO + CH_3OO \rightarrow nC_4H_9OH + HCHO$	2.3×10^{-13}	Michalowski et al. (2000)
$CH_3OH + OH \rightarrow CH_3O$	7.09×10^{-13}	Atkinson et al. (2004)
n-Butanal $+ OH \rightarrow$ Products	2.0×10^{-11}	Michalowski et al. (2000)
$CH_3OO + HO_2 \rightarrow CH_3OOH$	8.82×10^{-12}	Atkinson et al. (2004)
$C_2H_5OO + HO_2 \rightarrow C_2H_5OOH$	1.12×10^{-11}	Atkinson et al. (2004)
$CH_3COOO + HO_2 \rightarrow CH_3COOOH$	2.54×10^{-11}	DeMore et al. (1997)
$C_2H_5OOH + OH \rightarrow C_2H_5OO$	6.0×10^{-12}	Atkinson et al. (2004)
$CH_3OO + CH_3OO \rightarrow HCHO + HO_2$	3.64×10^{-13}	Lurmann et al. (1986)
$CH_3OOH + OH \rightarrow HCHO + H_2O + OH$	2.54×10^{-12}	Sander and Crutzen (1996)
$CH_3OOH + OH \rightarrow CH_3OO + H_2O$	6.01×10^{-12}	Sander and Crutzen (1996)
$CH_3OO + HO_2 \rightarrow CH_3OOH$	1.01×10^{-11}	Atkinson et al. (2004)
$CH_3OO + NO \rightarrow HCHO + HO_2 + NO_2$	8.76×10^{-12}	Atkinson et al. (2004)
$CH_3OO + nC_3H_7O_2 \rightarrow HCHO + C_3H_6O + HO_2 + HO_2$	6.70×10^{-13}	Lightfoot et al. (1992)
$CH_3OO + nC_3H_7O_2 \rightarrow C_3H_6O + CH_3OH$	2.3×10^{-13}	Lightfoot et al. (1992)
$CH_3OO + nC_3H_7O_2 \rightarrow HCHO + nC_3H_7OH$	2.3×10^{-13}	Lightfoot et al. (1992)
$CH_3OO + iC_3H_7O_2 \rightarrow HCHO + CH_3COCH_3 + HO_2 + HO_2$	1.2×10^{-14}	Lightfoot et al. (1992)
$CH_3OO + iC_3H_7O_2 \rightarrow CH_3COCH_3 + CH_3OH$	4.1×10^{-15}	Lightfoot et al. (1992)
$CH_3OO + iC_3H_7O_2 \rightarrow HCHO + iC_3H_7OH$	4.1×10^{-15}	Lightfoot et al. (1992)
$CH_3OO + C_2H_5OO \rightarrow CH_3CHO + HCHO + HO_2 + HO_2$	2.0×10^{-13}	Kirchner and Stockwell (1996)
$CH_3OO + CH_3COOO \rightarrow HCHO + CH_3OO + HO_2$	1.58×10^{-11}	Kirchner and Stockwell (1996)
$C_2H_5OO + NO \rightarrow CH_3CHO + HO_2 + NO_2$	8.68×10^{-12}	Lurmann et al. (1986)
$C_2H_5OO + HO_2 \rightarrow C_2H_5OOH$	9.23×10^{-12}	Atkinson et al. (2004)
$C_2H_5OO + CH_3COOO \rightarrow CH_3CHO + CH_3COO + HO_2$	4.0×10^{-12}	Michalowski et al. (2000)
$iC_3H_7O_2 + HO_2 \rightarrow$ *i*Perox	9.23×10^{-12}	Michalowski et al. (2000)
$nC_3H_7O_2 + HO_2 \rightarrow$ *n*Perox	9.23×10^{-12}	Michalowski et al. (2000)
$HCHO + OH \rightarrow HO_2 + CO$	9.3×10^{-12}	Atkinson et al. (2004)
$HCHO + HO_2 \rightarrow HOCH_2O_2$	7.53×10^{-14}	Sander et al. (2006)

ACPD
14, 28685–28755, 2014

Table 1. Continued.

Reaction	Rate Constant	Reference
$HCHO + NO_3 \rightarrow HNO_3 + HO_2 + CO$	5.8×10^{-16}	DeMore et al. (1997)
$CH_3CHO + OH \rightarrow CH_3COOO + H_2O$	1.98×10^{-11}	Atkinson et al. (2004)
$CH_3CHO + NO_3 \rightarrow HNO_3 + CH_3COOO$	1.4×10^{-15}	DeMore et al. (1997)
$CH_3COCH_3 + OH \rightarrow H_2O + CH_3COCH_2$	1.37×10^{-13}	Atkinson et al. (2004)
$HOCH_2O_2 + NO \rightarrow HCOOH + HO_2 + NO_2$	8.68×10^{-12}	Lurmann et al. (1986)
$HOCH_2O_2 + HO_2 \rightarrow HCOOH + H_2O$	2.0×10^{-12}	Lurmann et al. (1986)
$HOCH_2O_2 + HOCH_2O_2 \rightarrow HCOOH + HCOOH + HO_2 + HO_2$	1.0×10^{-13}	Lurmann et al. (1986)
$HCOOH + OH \rightarrow HO_2 + H_2O + CO_2$	4.0×10^{-13}	DeMore et al. (1997)
$CH_3COOO + NO \rightarrow CH_3OO + NO_2 + CO_2$	2.4×10^{-11}	Atkinson et al. (2004)
$CH_3COOO + HO_2 \rightarrow CH_3COOH + O_3$	1.87×10^{-11}	Kirchner and Stockwell (1996)
$CH_3COOO + CH_3COOO \rightarrow CH_3COO + CH_3COO$	2.5×10^{-11}	Kirchner and Stockwell (1996)
$Cl_2 + OH \rightarrow HOCl + Cl$	2.85×10^{-14}	Atkinson et al. (2004)
$Cl + O_3 \rightarrow ClO$	1.02×10^{-11}	Atkinson et al. (2004)
$Cl + H_2 \rightarrow HCl$	3.5×10^{-15}	Atkinson et al. (2004)
$Cl + HO_2 \rightarrow HCl$	3.57×10^{-11}	Sander et al. (2006)
$Cl + HO_2 \rightarrow ClO + OH$	6.68×10^{-12}	Sander et al. (2006)
$Cl + H_2O_2 \rightarrow HCl + HO_2$	2.11×10^{-13}	Atkinson et al. (2004)
$Cl + NO_3 \rightarrow ClO + NO_2$	2.4×10^{-11}	Atkinson et al. (2004)
$Cl + CH_4 \rightarrow HCl + CH_3OO$	3.99×10^{-14}	Sander et al. (2006)
$Cl + C_2H_6 \rightarrow HCl + C_2H_5OO$	5.36×10^{-11}	Sander et al. (2006)
$Cl + C_2H_4 \rightarrow HCl + C_2H_5OO$	1.0×10^{-10}	Atkinson et al. (2004)
$Cl + MEK \rightarrow HCl$	4.21×10^{-11}	Atkinson et al. (2004)
$Cl + C_2H_2 \rightarrow ClC_2CHO$	2.5×10^{-10}	Atkinson et al. (2004)
$Cl + C_3H_6 \rightarrow HCl + C_3H_6Cl$	2.7×10^{-10}	Keil and Shepson (2006)
$Cl + C_3H_8 \rightarrow HCl + iC_3H_7O_2$	1.65×10^{-10}	DeMore et al. (1997)
$Cl + C_3H_8 \rightarrow HCl + nC_3H_7O_2$	1.65×10^{-10}	DeMore et al. (1997)
$Cl + C_3H_6O \rightarrow HCl$	1.1×10^{-10}	Wallington et al. (1988)
$Cl + iC_4H_{10} \rightarrow HCl + C_4H_9$	1.3×10^{-10}	Hooshiyar and Niki (1995)
$Cl + nC_4H_{10} \rightarrow HCl + C_4H_9$	2.15×10^{-10}	Tyndall et al. (1997)
Cl + n-Butanal → HCl + Products	1.1×10^{-10}	Michalowski et al. (2000)
$Cl + HCHO \rightarrow HCl + HO_2 + CO$	7.18×10^{-11}	Sander et al. (2003)
$Cl + CH_3CHO \rightarrow HCl + CH_3COOO$	8.08×10^{-11}	Atkinson et al. (2004)
$Cl + CH_3COCH_3 \rightarrow HCl + CH_3COCH_2$	1.39×10^{-12}	Atkinson et al. (2004)
$Cl + CH_3OOH \rightarrow CH_3OO + HCl$	2.36×10^{-11}	Atkinson et al. (2004)
$Cl + CH_3OOH \rightarrow CH_2OOH + HCl$	3.54×10^{-11}	Atkinson et al. (2004)
$Cl + CHBr_3 \rightarrow HCl + Br + CBr_2O$	2.9×10^{-13} (at 298 K)	Kamboures et al. (2002)
$Cl + OClO \rightarrow ClO + ClO$	6.35×10^{-11}	Atkinson et al. (2004)

ACPD
14, 28685–28755, 2014

Table 1. Continued.

Reaction	Rate Constant	Reference
$Cl + ClNO_3 \rightarrow Cl_2 + NO_3$	1.12×10^{-11}	Sander et al. (2006)
$Cl + PAN \rightarrow HCl + HCHO + NO_3$	1.0×10^{-14}	Tsalkani et al. (1988)
$Cl + HNO_3 \rightarrow HCl + NO_3$	1.0×10^{-16}	Wine et al. (1988)
$Cl + NO_2 \rightarrow ClNO_2$	1.43×10^{-12} (at 298 K)	Ravishankara et al. (1988)
$Cl + HBr \rightarrow HCl + Br$	4.48×10^{-12}	Nicovich and Wine (2004)
$ClO + O(^3P) \rightarrow Cl + O_2$	1.6×10^{-11}	Atkinson et al. (2004)
$ClO + OH \rightarrow Cl + HO_2$	2.45×10^{-11}	Atkinson et al. (2004)
$ClO + OH \rightarrow HCl$	2.37×10^{-13}	Sander et al. (2006)
$ClO + HO_2 \rightarrow HOCl$	8.67×10^{-12}	Atkinson et al. (2004)
$ClO + CH_3OO \rightarrow Cl + HCHO + HO_2$	2.08×10^{-12}	Sander et al. (2006)
$ClO + CH_3COOO \rightarrow Cl + CH_3OO + CO_2$	2.03×10^{-12}	Michalowski et al. (2000)
$ClO + NO \rightarrow Cl + NO_2$	2.04×10^{-11}	Atkinson et al. (2004)
$ClO + NO_2 \rightarrow ClNO_3$	7.1×10^{-12}	Atkinson et al. (2004)
$ClO + ClO \rightarrow Cl_2$	1.64×10^{-15}	Atkinson et al. (2004)
$ClO + ClO \rightarrow Cl + Cl$	1.54×10^{-15}	Atkinson et al. (2004)
$ClO + ClO \rightarrow Cl + OclO$	1.40×10^{-15}	Atkinson et al. (2004)
$OclO + OH \rightarrow HOCl$	1.13×10^{-11}	Atkinson et al. (2004)
$OclO + NO \rightarrow ClO + H_2O$	1.51×10^{-13}	Atkinson et al. (2004)
$HOCl + OH \rightarrow ClO + H_2O$	4.0×10^{-13}	Sander et al. (2006)
$HCl + OH \rightarrow Cl + H_2O$	6.84×10^{-13}	Atkinson et al. (2004)
$ClNO_3 + OH \rightarrow HOCl + NO_3$	3.17×10^{-13}	Atkinson et al. (2004)
$HOCl + O(^3P) \rightarrow ClO + OH$	1.7×10^{-13}	Atkinson et al. (2004)
$Br + O_3 \rightarrow BrO$	6.75×10^{-13}	Atkinson et al. (2004)
$Br_2 + OH \rightarrow HOBr$	5.0×10^{-11}	Atkinson et al. (2004)
$Br + HO_2 \rightarrow HBr$	1.25×10^{-12}	Atkinson et al. (2004)
$Br + C_2H_2 \rightarrow BrCH_2CHO$	3.7×10^{-14}	Atkinson et al. (2004)
$Br + C_2H_4 \rightarrow HBr + C_2H_5OO$	1.3×10^{-13}	Atkinson et al. (2004)
$Br + C_3H_6 \rightarrow HBr + C_3H_5$	1.60×10^{-12}	Atkinson et al. (2004)
$Br + HCHO \rightarrow HBr + CO + HO_2$	6.75×10^{-13}	Sander et al. (2006)
$Br + CH_3CHO \rightarrow HBr + CH_3COOO$	2.8×10^{-12}	Atkinson et al. (2004)
$Br + C_3H_6O \rightarrow HBr$	9.7×10^{-12}	Wallington et al. (1989)
$Br + n-Butanal \rightarrow HBr$	9.7×10^{-12}	Michalowski et al. (2000)
$Br + CH_3OOH \rightarrow HBr + CH_3OO$	4.03×10^{-15}	Mallard et al. (1993)
$Br + NO_2 \rightarrow BrNO_2$	2.7×10^{-11}	Atkinson et al. (2004)
$Br + BrNO_3 \rightarrow Br_2 + NO_3$	4.9×10^{-11}	Orlando and Tyndall (1997)
$Br + OclO \rightarrow BrO + ClO$	1.43×10^{-13}	Atkinson et al. (2004)
$BrO + O(^3P) \rightarrow Br$	4.8×10^{-11}	Atkinson et al. (2004)

ACPD
14, 28685–28755, 2014

Table 1. Continued.

Reaction	Rate Constant	Reference
$BrO + OH \rightarrow Br + HO_2$	4.93×10^{-11}	Atkinson et al. (2004)
$BrO + HO_2 \rightarrow HOBr$	3.38×10^{-11}	Atkinson et al. (2004)
$BrO + CH_3OO \rightarrow HOBr + CH_2OO$	4.1×10^{-12}	Aranda et al. (1997)
$BrO + CH_3OO \rightarrow Br + HCHO + HO_2$	1.6×10^{-12}	Aranda et al. (1997)
$BrO + CH_3COOO \rightarrow Br + CH_3COO$	1.7×10^{-12}	Michalowski et al. (2000)
$BrO + C_3H_6O \rightarrow HOBr$	1.5×10^{-14}	Michalowski et al. (2000)
$BrO + NO \rightarrow Br + NO_2$	2.48×10^{-11}	Atkinson et al. (2004)
$BrO + NO_2 \rightarrow BrNO_3$	1.53×10^{-11}	Atkinson et al. (2004)
$BrO + BrO \rightarrow Br + Br$	2.82×10^{-12}	Sander et al. (2006)
$BrO + BrO \rightarrow Br_2$	9.3×10^{-13}	Sander et al. (2006)
$BrO + HBr \rightarrow HOBr + Br$	2.1×10^{-14}	Hansen et al. (1999)
$HBr + OH \rightarrow Br + H_2O$	1.26×10^{-11}	Sander et al. (2006)
$CH_3Br + OH \rightarrow H_2O + Br$	1.27×10^{-14}	Atkinson et al. (2004)
$CHBr_3 + OH \rightarrow H_2O + Br$	1.2×10^{-13}	Atkinson et al. (2004)
$Cl + BrCl \leftrightarrow Br + Cl_2$	$f: 1.5 \times 10^{-11}$ $r: 1.1 \times 10^{-15}$	Clyne and Cruse (1972)
$Cl + Br_2 \leftrightarrow BrCl + Br$	$f: 1.2 \times 10^{-10}$ $r: 3.3 \times 10^{-1}$	Clyne and Cruse (1972)
$BrO + ClO \rightarrow Br + Cl$	7.04×10^{-12}	Atkinson et al. (2004)
$BrO + ClO \rightarrow BrCl$	1.15×10^{-12}	Atkinson et al. (2004)
$BrO + ClO \rightarrow Br + OclO$	9.06×10^{-12}	Atkinson et al. (2004)
$HOBr + OH \rightarrow BrO + H_2O$	5.0×10^{-13}	Kukui et al. (1996)
$HOBr + Cl \rightarrow BrCl + OH$	8.0×10^{-11}	Kukui et al. (1996)
$HOBr + O(^3P) \rightarrow BrO + OH$	2.12×10^{-11}	Atkinson et al. (2004)
$I_2 + O(^3P) \rightarrow IO + I$	1.25×10^{-10} (at 298 K)	Atkinson et al. (2004)
$IO + O(^3P) \rightarrow I$	1.4×10^{-10} (at 298 K)	Atkinson et al. (2004)
$I + HO_2 \rightarrow HI$	1.85×10^{-13}	Atkinson et al. (2004)
$I + O_3 \rightarrow IO$	7.39×10^{-13}	Atkinson et al. (2004)
$I + NO \rightarrow INO$	3.48×10^{-13} (at 298 K)	Atkinson et al. (2004)
$I + NO_2 \rightarrow INO_2$	5.76×10^{-12} (at 298 K)	Atkinson et al. (2004)
$I + NO_3 \rightarrow IO + NO_3$	1.0×10^{-10} (at 298 K)	Atkinson et al. (2004)
$I_2 + NO_3 \rightarrow I + IONO_2$	1.5×10^{-12} (at 298 K)	Atkinson et al. (2004)
$HI + OH \rightarrow I + H_2O$	9.43×10^{-11}	Atkinson et al. (2004)
$I_2 + OH \rightarrow HOI + I$	2.1×10^{-10}	Atkinson et al. (2004)
$IO + NO_3 \rightarrow OIO + NO_2$	9.0×10^{-12} (at 298 K)	Atkinson et al. (2004)
$IO + HO_2 \rightarrow HOI$	8.4×10^{-11} (at 298 K)	Atkinson et al. (2004)

ACPD
14, 28685–28755, 2014

Table 1. Continued.

Reaction	Rate Constant	Reference
$IO + ClO \rightarrow Icl$	3.16×10^{-12}	Turnipseed et al. (1997)
$IO + ClO \rightarrow I + Cl$	3.95×10^{-12}	Turnipseed et al. (1997)
$IO + ClO \rightarrow I + OclO$	8.69×10^{-12}	Turnipseed et al. (1997)
$IO + BrO \rightarrow Br + OIO$	9.36×10^{-11}	Rowley et al. (2001)
$IO + BrO \rightarrow Ibr$	4.32×10^{-11}	Rowley et al. (2001)
$IO + BrO \rightarrow Br + I$	7.2×10^{-12}	Rowley et al. (2001)
$IO + IO \rightarrow I + OIO$	4.41×10^{-11}	Atkinson et al. (2004)
$IO + IO \rightarrow I + I$	1.84×10^{-11}	Atkinson et al. (2004)
$IO + IO \leftrightarrow IOOI$	$f: 5.34 \times 10^{-11}$ $r: 1.3 \times 10^{-4}$	Atkinson et al. (2004)
$IOOI \rightarrow OIO + I$	0.21	Saiz-Lopez et al. (2008)
$IO + NO \rightarrow I + NO_2$	1.96×10^{-11}	Atkinson et al. (2004)
$IO + NO_2 \leftrightarrow IONO_2$	$f: 4.61 \times 10^{-11}$ $r: 8.36 \times 10^{-7}$	Atkinson et al. (2004)
$OIO + NO \rightarrow IO + NO_2$	9.78×10^{-12}	Atkinson et al. (2004)
$OIO + OH \rightarrow HOI$	6.0×10^{-12}	McFiggans et al. (2002)
$HOI + OH \rightarrow IO$	2.0×10^{-13}	McFiggans et al. (2002)
$IO + OIO \rightarrow I_2O_3$	1.5×10^{-10}	Gomez Martin et al. (2005)
$OIO + OIO \leftrightarrow I_2O_4$	$f: 1.0 \times 10^{-10}$ $r: 4.4 \times 10^{-4}$	Sander et al. (2006)
$IOOI + O_3 \rightarrow I_2O_3$	1.0×10^{-12}	Saunders and Plane (2006)
$I_2O_3 + O_3 \rightarrow I_2O_4$	1.0×10^{-12}	Saunders and Plane (2006)
$I_2O_4 + O_3 \rightarrow I_2O_5$	1.0×10^{-12}	Saunders and Plane (2006)

ACPD
14, 28685–28755, 2014

Table 2. Photochemical reactions. J_{max} values for 25 March are shown as an example. J coefficients are expressed in units of s^{-1}.

Reaction	J_{max} 25 March	Lifetime	Source
$O_3 \rightarrow O_2 + O(^1D)$	3.9×10^{-6}	3.0 days	calculated from OASIS data
$NO_2 \rightarrow NO + O(^3P)$	8.6×10^{-3}	1.9 min	calculated from OASIS data
$H_2O_2 \rightarrow OH + OH$	3.4×10^{-6}	3.4 days	calculated from OASIS data
$NO_3 \rightarrow NO + O_2$	4.5×10^{-2}	22 s	Michalowski et al. (2000)
$N_2O_5 \rightarrow NO_2 + NO_3$	1.5×10^{-5}	18 h	calculated from OASIS data
$HONO \rightarrow OH + NO$	1.8×10^{-3}	9.2 min	calculated from OASIS data
$HNO_3 \rightarrow NO_2 + OH$	1.5×10^{-7}	79 days	calculated from OASIS data
$HNO_4 \rightarrow NO_2 + HO_2$	7.3×10^{-7}	16 days	calculated from OASIS data
$HCHO \rightarrow HO_2 + HO_2 + CO$	1.5×10^{-5}	19 h	calculated from OASIS data
$HCHO \rightarrow CO + H_2$	3.1×10^{-5}	8.8 h	calculated from OASIS data
$CH_3CHO \rightarrow CH_3OO + HO_2 + CO$	1.1×10^{-6}	11 days	calculated from OASIS data
$CH_3OOH \rightarrow HCHO + HO_2 + OH$	3.2×10^{-6}	3.7 days	calculated from OASIS data
$C_3H_6O \rightarrow HO_2 + C_2H_5OO + CO$	1.4×10^{-6}	8.3 days	calculated from OASIS data
$PAN \rightarrow CH_3COOO + NO_2$	1.7×10^{-7}	66 days	calculated from OASIS data
$OClO \rightarrow O(^3P) + ClO$	0.12	8.1 s	estimate from Pöhler et al. (2010)
$Cl_2 \rightarrow Cl + Cl$	2.1×10^{-3}	8.1 min	calculated from OASIS data
$ClO \rightarrow Cl + O(^3P)$	2.4×10^{-5}	11 h	calculated from OASIS data
$HOCl \rightarrow OH + Cl$	1.4×10^{-4}	2 h	estimate from Lehrer et al. (2004)
$ClNO_3 \rightarrow Cl + NO_3$	2.9×10^{-5}	9.5 h	calculated from OASIS data
$ClNO_3 \rightarrow ClO + NO_2$	3.4×10^{-6}	3.4 days	calculated from OASIS data
$BrNO_3 \rightarrow Br + NO_3$	2.1×10^{-4}	1.3 h	calculated from OASIS data
$BrNO_3 \rightarrow BrO + NO_2$	1.2×10^{-3}	14.2 min	calculated from OASIS data
$BrO \rightarrow Br + O(^3P)$	3.0×10^{-2}	33 s	calculated from OASIS data
$Br_2 \rightarrow Br + Br$	4.4×10^{-2}	23 s	calculated from OASIS data
$HOBr \rightarrow Br + OH$	2.3×10^{-3}	7.2 min	calculated from OASIS data
$BrNO_2 \rightarrow Br + NO_2$	1.5×10^{-4}	1.8 h	estimate from Lehrer et al. (2004)
$ClNO_2 \rightarrow Cl + NO_2$	4.4×10^{-5}	6.3 h	estimate from Ganske et al. (1992)
$BrCl \rightarrow Br + Cl$	1.26×10^{-2}	1.3 min	calculated from OASIS data
$I_2 \rightarrow I + I$	0.15	6.7 s	calculated from Calvert and Lindberg (2004)
$ICl \rightarrow I + Cl$	2.21×10^{-2}	45 s	calculated from Calvert and Lindberg (2004)
$IBr \rightarrow I + Br$	6.83×10^{-2}	14.6 s	calculated from Calvert and Lindberg (2004)
$INO_2 \rightarrow I + NO_2$	2.23×10^{-3}	7.5 min	calculated from Calvert and Lindberg (2004)
$INO \rightarrow I + NO$	8.34×10^{-2}	12 s	calculated from Calvert and Lindberg (2004)
$IONO_2 \rightarrow IO + NO_2$	7.13×10^{-4}	23.4 min	calculated from Calvert and Lindberg (2004)
$IONO_2 \rightarrow I + NO_3$	2.91×10^{-4}	57.3 min	calculated from Calvert and Lindberg (2004)
$IOOI \rightarrow I + I$	1.50×10^{-2}	66.7 s	calculated from Calvert and Lindberg (2004)
$IOOI \rightarrow IO + IO$	1.50×10^{-2}	66.7 s	calculated from Calvert and Lindberg (2004)
$HOI \rightarrow I + OH$	5.09×10^{-3}	3.3 min	calculated from Calvert and Lindberg (2004)
$IO \rightarrow I + O(^3P)$	0.18	5.6 s	calculated from Calvert and Lindberg (2004)
$OIO \rightarrow IO + O(^3P)$	1.52×10^{-3}	11 min	calculated from Calvert and Lindberg (2004)
$OIO \rightarrow I$	3.26×10^{-2}	30.7 s	calculated from Calvert and Lindberg (2004)

ACPD
14, 28685–28755, 2014

Table 3. Mass transfer reactions. All rate constants are expressed in units of s^{-1}.

Reaction	k (forward)	k (reverse)
Particles		
$HCl_{(g)} \rightarrow H^+_{(p)} + Cl^-_{(p)}$	2.58×10^{-3}	
$HBr_{(g)} \rightarrow H^+_{(p)} + Br^-_{(p)}$	1.80×10^{-3}	
$HOCl_{(g)} \rightarrow HOCl_{(p)}$	2.16×10^{-3}	
$HOBr_{(g)} \rightarrow HOBr_{(p)}$	1.26×10^{-3}	
$HOI_{(g)} \rightarrow HOI_{(p)}$	5.42×10^{-4}	
$OH_{(g)} \rightarrow OH_{(p)}$	3.26×10^{-5}	
$O_{3(g)} \leftrightarrow O_{3(p)}$	6.54×10^{-6}	8.76×10^{5}
$Cl_{2(g)} \leftrightarrow Cl_{2(p)}$	2.69×10^{-5}	2.96×10^{7}
$Br_{2(g)} \leftrightarrow Br_{2(p)}$	1.78×10^{-5}	2.97×10^{8}
$BrCl_{(g)} \leftrightarrow BrCl_{(p)}$	6.60×10^{-4}	1.91×10^{10}
$Icl_{(p)} \rightarrow Icl_{(g)}$	2.83×10^{10}	
$Ibr_{(p)} \rightarrow Ibr_{(g)}$	5.53×10^{9}	
$HNO_{3(g)} \rightarrow HNO_{3(p)}$	5.50×10^{-4}	
$N_2O_{5(g)} \rightarrow N_2O_{5(p)}$	1.08×10^{-4}	
$HONO_{(g)} \rightarrow HONO_{(p)}$	1.63×10^{-4}	
$PAN_{(g)} \rightarrow PAN_{(p)}$	2.05×10^{-5}	
$HNO_{4(g)} \rightarrow HNO_{4(p)}$	4.89×10^{-4}	
$ClNO_{2(p)} \rightarrow ClNO_{2(g)}$	9.44×10^{3}	
$BrNO_{2(p)} \rightarrow BrNO_{2(g)}$	4.94×10^{4}	
Snow		
$HBr_{(g)} \rightarrow H^+_{(s)} + Br^-_{(s)}$	1.67×10^{-5}	
$HCl_{(g)} \rightarrow H^+_{(s)} + Cl^-_{(s)}$	1.67×10^{-5}	
$HOBr_{(g)} \rightarrow HOBr_{(s)}$	1.67×10^{-5}	
$HOCl_{(g)} \rightarrow HOCl_{(s)}$	1.67×10^{-5}	
$HOI_{(g)} \rightarrow HOI_{(s)}$	1.67×10^{-5}	
$OH_{(g)} \rightarrow OH_{(s)}$	1.67×10^{-6}	
$O_{3(g)} \rightarrow O_{3(s)}$	1.67×10^{-6}	
$Cl_{2(g)} \leftrightarrow Cl_{2(s)}$	8.0×10^{-6}	7.71×10^{-2}
$Br_{2(g)} \leftrightarrow Br_{2(s)}$	1.0×10^{-5}	7.71×10^{-2}
$BrCl_{(g)} \leftrightarrow BrCl_{(s)}$	1.25×10^{-5}	7.71×10^{-2}
$Icl_{(s)} \rightarrow Icl_{(g)}$	7.71×10^{-2}	
$Ibr_{(s)} \rightarrow Ibr_{(g)}$	7.71×10^{-2}	
$HNO_{3(g)} \rightarrow HNO_{3(s)}$	1.67×10^{-5}	
$N_2O_{5(g)} \rightarrow N_2O_{5(s)}$	1.67×10^{-5}	
$HONO_{(g)} \rightarrow HONO_{(s)}$	1.67×10^{-5}	
$PAN_{(g)} \rightarrow PAN_{(s)}$	1.67×10^{-5}	
$HNO_{4(g)} \rightarrow HNO_{4(s)}$	1.67×10^{-5}	
$ClNO_{2(s)} \rightarrow ClNO_{2(g)}$	7.71×10^{-2}	
$BrNO_{2(s)} \rightarrow BrNO_{2(g)}$	7.71×10^{-2}	

ACPD
14, 28685–28755, 2014

Table 4. Aqueous-phase reactions in the model. All aqueous reaction rate constants are converted to units consistent to the gas-phase reactions to be read by the modeling program.

Reaction	k (actual)	k (particle)	k (snow)	Reference
$Cl^- + HOBr + H^+ \rightarrow BrCl$[1]	1.55×10^{-32}	5.17×10^{-21}	9.30×10^{-26}	Wang et al. (1994)
$Br^- + HOCl + H^+ \rightarrow BrCl$[1]	3.59×10^{-36}	1.2×10^{-24}	2.15×10^{-29}	Sander et al. (1997)
$Br^- + HOBr + H^+ \rightarrow Br_2$[1]	4.41×10^{-32}	1.47×10^{-20}	2.64×10^{-25}	Beckwith et al. (1996)
$Cl^- + HOCl + H^+ \rightarrow Cl_2$[1]	6.07×10^{-38}	2.02×10^{-26}	3.63×10^{-31}	Wang and Margerum (1994)
$Cl^- + HOI + H^+ \rightarrow ICl$[1]	8.01×10^{-32}	2.67×10^{-20}	4.80×10^{-25}	Wang et al. (1989)
$Br^- + HOI + H^+ \rightarrow IBr$[1]	9.12×10^{-30}	3.04×10^{-18}	5.46×10^{-23}	Troy et al. (1991)
$BrCl + Cl^- \rightarrow BrCl_2^-$[2]	1×10^{-11}	3.3	5.99×10^{-5}	Michalowski et al. (2000)
$BrCl_2^- \rightarrow BrCl + Cl^-$[3]	1.58×10^{9}	1.58×10^{9}	1.58×10^{9}	Michalowski et al. (2000)
$BrCl + Br^- \rightarrow Br_2Cl^-$[2]	1×10^{-11}	3.3	5.99×10^{-5}	Michalowski et al. (2000)
$Br_2Cl^- \rightarrow BrCl + Br^-$[3]	3.34×10^{5}	3.34×10^{5}	3.34×10^{5}	Wang et al. (1994); Michalowski et al. (2000)
$Cl_2 + Br^- \rightarrow BrCl_2^-$[2]	1.28×10^{-11}	4.27	7.66×10^{-5}	Wang et al. (1994); Michalowski et al. (2000)
$BrCl_2^- \rightarrow Cl_2 + Br^-$[3]	6.94×10^{2}	6.94×10^{2}	6.94×10^{2}	Wang et al. (1994); Michalowski et al. (2000)
$O_3 + Br^- \rightarrow HOBr$[2]	1.35×10^{-20}	4.5×10^{-9}	8.08×10^{-14}	Oum et al. (1998); Michalowski et al. (2000)
$OH + Cl^- \rightarrow HOCl$[2]	1.35×10^{-20}	4.5×10^{-9}	8.08×10^{-14}	assumed same as $O_3 + Br^-$
$N_2O_5 + Cl^- \rightarrow ClNO_2$[2]	1.66×10^{-12}	5.5×10^{-1}	9.94×10^{-5}	assume diffusion limited
$ClNO_2 + H^+ + Cl^- \rightarrow Cl_2$[2]	1.66×10^{-14}	5.5×10^{-3}	9.94×10^{-8}	estimated from Roberts et al. (2008)
$N_2O_5 + Br^- \rightarrow BrNO_2$[2]	1.66×10^{-12}	5.5×10^{-1}	9.94×10^{-5}	assume diffusion limited
$BrNO_2 + H^+ + Br^- \rightarrow Br_2$[2]	7.31×10^{-17}	2.44×10^{-5}	4.38×10^{-10}	estimated from Schweitzer et al. (1998)

[1] Third order rate constant, expressed in units of $cm^6\ molecule^{-2}\ s^{-1}$
[2] second order rate constant, expressed in units of $cm^3\ molecule^{-1}\ s^{-1}$
[3] first order rate constant, expressed in units of s^{-1}

ACPD
14, 28685–28755, 2014

Table 5. Summary of the ambient measurements from OASIS that were used to constrain the model and the instrumental method used.

Measured Species	Method	Method Reference
O_3, NO_2	Chemiluminescence	Ridley et al. (1992); Ryerson et al. (2000)
CO	CO Monitor	
Cl_2, Br_2, BrO, HOBr	CIMS	Liao et al. (2011, 2012)
ClO	Chemical Reaction GC-ECD	Stephens et al. (2012)
HCHO	Tunable Diode Laser Absorption Spectroscopy	Fried et al., (1997); Lancaster et al. (2000)
CH_3CHO, CH_3COCH_3, MEK, n-C_4H_{10}, i-C_4H_{10}	Online GC-MS	Apel et al. (2010)
C_2H_2, C_2H_4, C_2H_6, C_3H_8, C_3H_6, n-C_4H_{10}, i-C_4H_{10}	Canister samples, offline GC-MS	Russo et al. (2010)

ACPD
14, 28685–28755, 2014

Table 6. Volumetric surface fluxes used in the model for NO_2, Br_2, HONO, and I_2. Fluxes in molecules $cm^{-2}\,s^{-1}$ are calculated using the effective mixing height, Z^*, following the method of Guimbaud et al., (2002). Z^* is calculated as $Z^* = \sqrt{(K_c \cdot \tau)}$, where K_c is the average atmospheric eddy diffusivity (95 $cm^2\,s^{-1}$), and τ is the atmospheric lifetime of the compound.

Compound	Model Flux (molecules $cm^{-3}\,s^{-1}$)	Z^* (m)	Flux (molecules $cm^{-2}\,s^{-1}$)
NO_2	variable, 1.0×10^5–3.0×10^6	1.0	1.0×10^7–3.0×10^8
Br_2	variable, 1.0×10^3–9.0×10^6	0.5	5.0×10^4–4.5×10^8
HONO	max 7.0×10^4, scaled to radiation	2.3	max 1.6×10^7
I_2	max 6.0×10^4, scaled to radiation	0.3	max 1.8×10^6

ACPD
14, 28685–28755, 2014

Table 7. Fraction of ozone depleted by each halogen calculated for mid-day of 25 March via Eq. (4). "Br and Cl" is the base model.

	Br Only	Br and Cl (base)	Br and I (1 ppt IO)	Br, Cl, and I (1 ppt IO)	Br, Cl, and I (0.5 ppt I_2)
% by Br	91 %	93 %	77 %	78 %	69 %
% by Cl		1.5 %		1.0 %	0.74 %
% by I			15 %	15 %	22 %
Total ΔO_3 (ppbv)	4.8	4.9	7.2	7.3	9.2

ACPD
14, 28685–28755, 2014

Table 8. Ozone depletion rates in ppb h^{-1} calculated by Eq. (3) and the corresponding timescale for ozone depletion for mid-day of day 25 Mar for six different modeling scenarios with different combinations of halogen radicals present. "Br and Cl" is the base model.

Model Conditions	Ozone Depletion Rate (ppb h^{-1})	Depletion Timescale (from 30 ppb)
Br Only	3.2	9.3 h
Cl Only	0.04	30 days
I Only (1 pptv IO)	0.76	1.6 days
I Only (0.5 pptv I_2)	1.6	19 h
Br and Cl (base)	3.4	8.7 h
Br and I (1 pptv IO)	5.2	5.8 h
Br, Cl, and I (1 pptv IO)	5.3	5.6 h
Br, Cl and I (0.5 pptv I_2)	6.6	4.5 h

ACPD
14, 28685–28755, 2014

Table 9. Ozone depletion rates in ppb h^{-1} calculated by Eq. (3) for mid-day of 25 Mar for six different modeling scenarios with varying [Cl_2]. The 16 pptv Cl_2 run is the base model.

Model Conditions	Ozone Depletion Rate (ppb h^{-1})	Depletion Timescale (from 30 ppb)
16 pptv Cl_2 (base)	3.4	8.7 h
100 pptv Cl_2	4.5	6.6 h
250 pptv Cl_2	8.6	3.5 h
400 pptv Cl_2	14	2.1 h

ACPD
14, 28685–28755, 2014

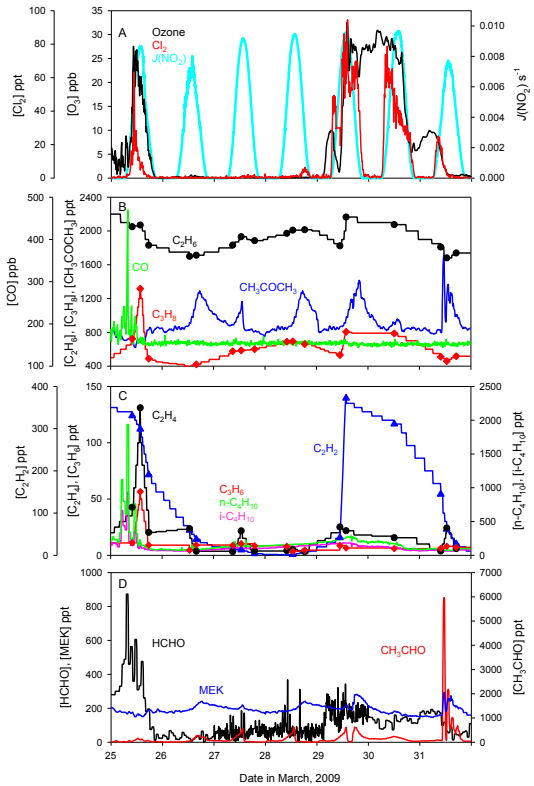

Figure 1. Ambient measurements of O_3, Cl_2, CO, VOCs, and OVOCs that are incorporated into the model. Mixing ratios for the NMHCs that were collected as canister samples were interpolated between samples. Available canister sample data points are indicated on their respective plot. Time is expressed in Alaska Standard Time. Radiation is plotted as the cyan trace in panel **(a)** as a reference.

ACPD
14, 28685–28755, 2014

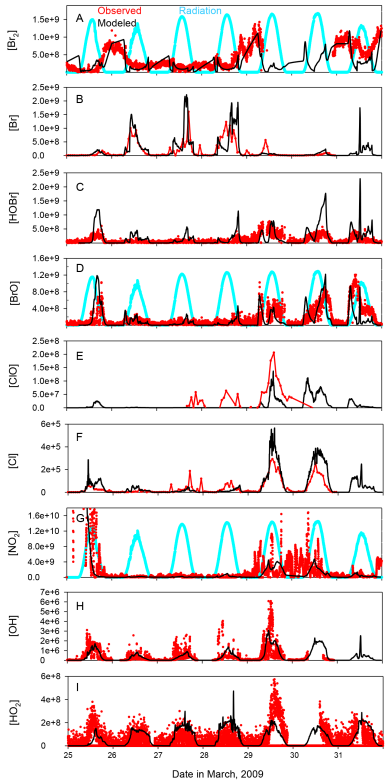

Figure 2. Modeled (black) compared to observed (red) time-series for Br_2, HOBr, BrO, ClO, NO_2, OH, and HO_2. The initial $[NO_2]$ is off the scale in order to clearly see the remaining data. Modeled Br and Cl (black) are compared to steady-state approximations as calculated in Stephens et al. (2012) (red). All concentrations are in molecules cm^{-3}. Radiation is shown as the cyan trace in select plots as a reference. Time is expressed in Alaska Standard Time.

ACPD
14, 28685–28755, 2014

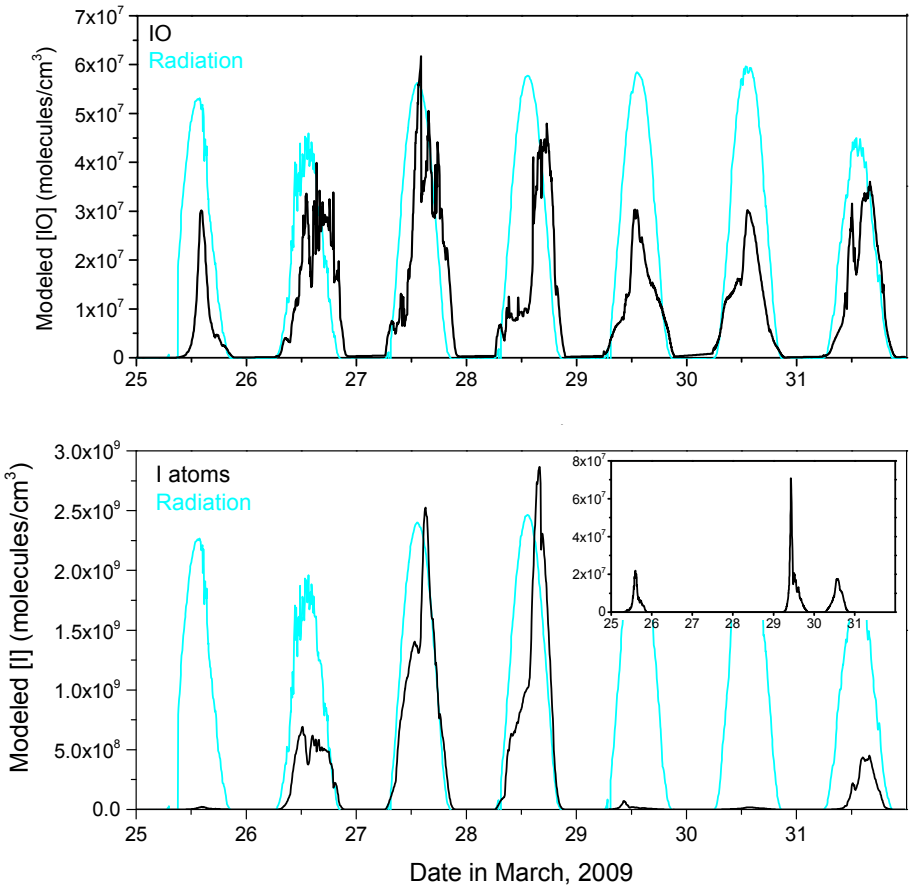

Figure 3. Modeled time-series of IO (top panel) and I atoms (bottom panel). Inset in bottom panel shows a close-up scaling of 25, 29, and 30 March. Radiation is shown as the cyan trace as a reference. Time is expressed in Alaska Standard Time.

ACPD
14, 28685–28755, 2014

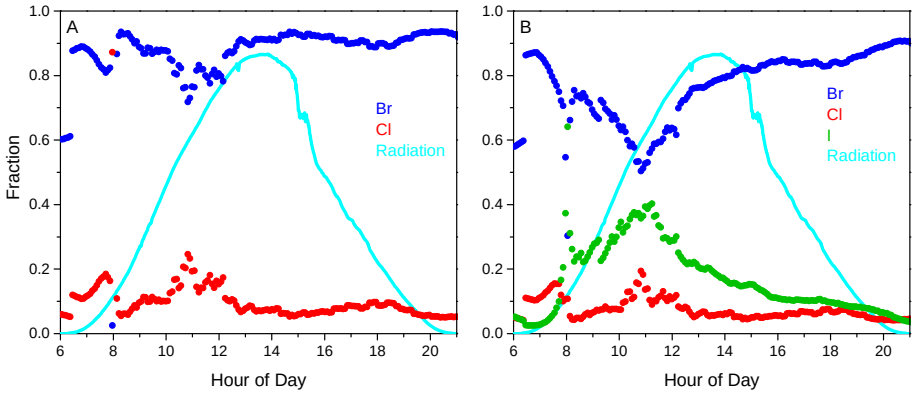

Figure 4. Average diurnal cycles of the fraction of O_3 depleted by Br and Cl **(a)** and Br, Cl, and I **(b)** for $[O_3] > 5$ ppbv. In both plots, Br is shown as the blue trace, Cl is the red trace, I is green trace, and radiation is shown as the cyan trace as a reference. Time is Alaska Standard Time.

ACPD
14, 28685–28755, 2014

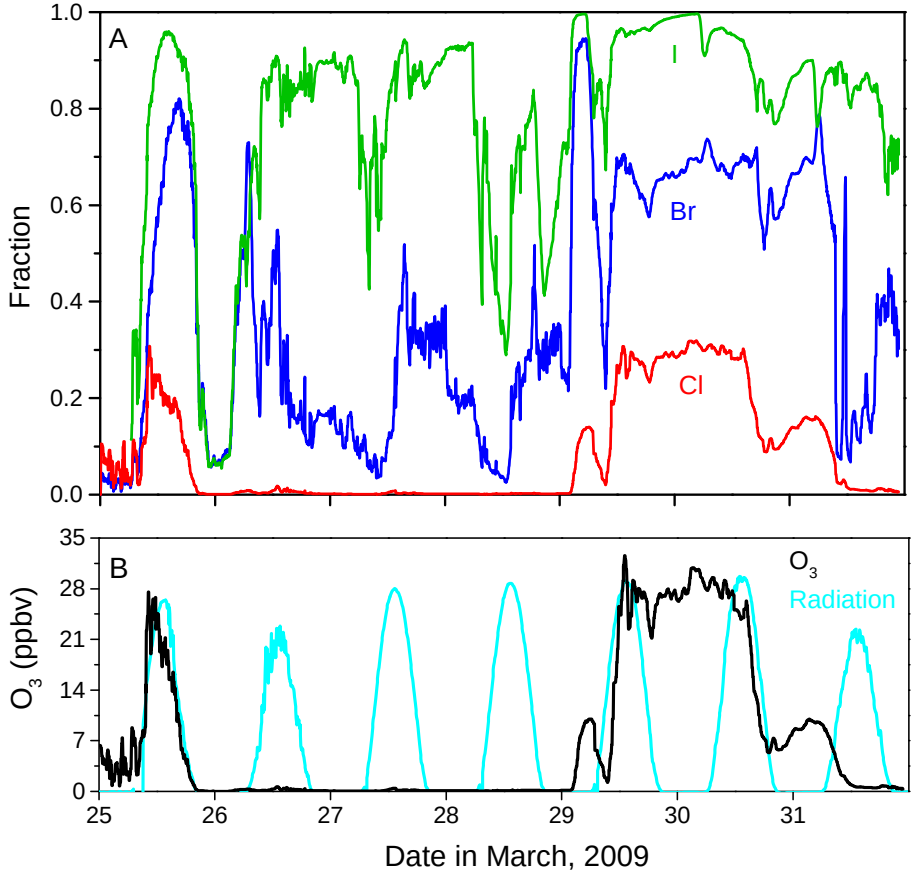

Figure 5. (a) Time-varying fraction of Br (blue), Cl (red), and I (green) atoms that react with O_3 across the 7 days of the simulation. **(b)** Time-series of observed ozone mole ratios, with radiation is shown as the cyan trace as a reference. Time is expressed in Alaska Standard Time.

ACPD
14, 28685–28755, 2014

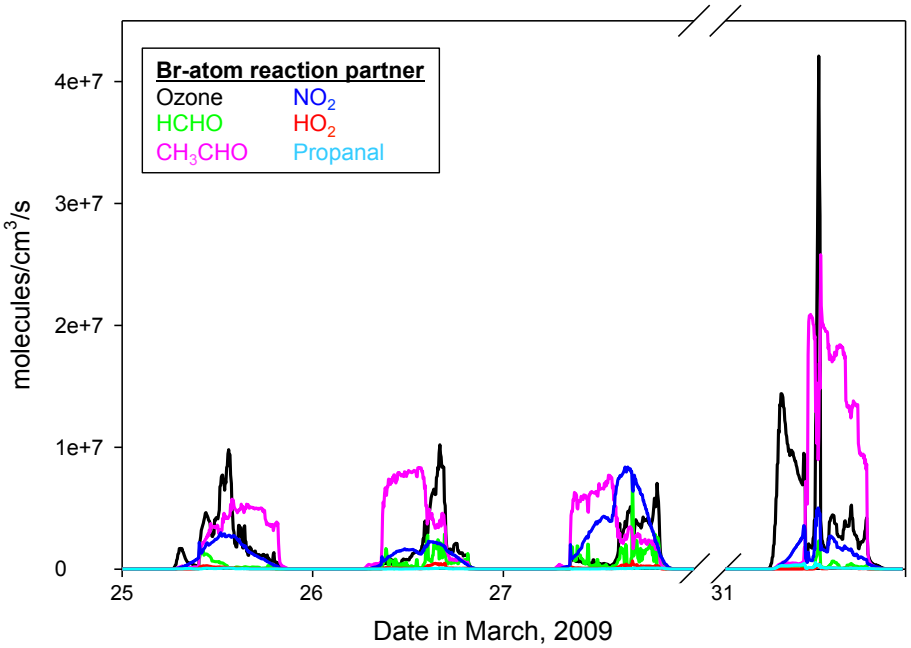

Figure 6. Time-varying rates (in molecules $cm^{-3}\,s^{-1}$) of the important Br atom sinks during ODEs ($[O_3] < 5$ ppb). Time is expressed in Alaska Standard Time.

ACPD
14, 28685–28755, 2014

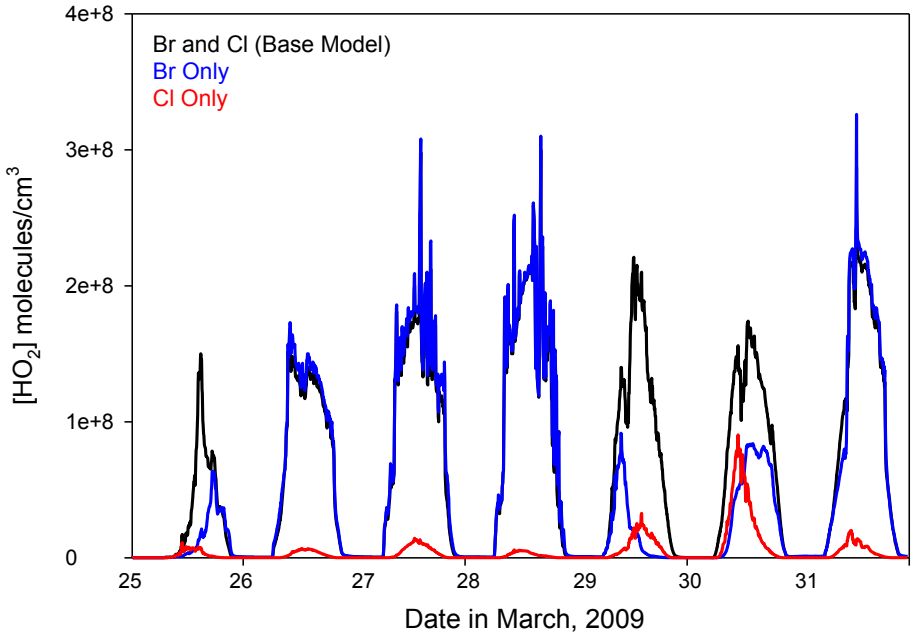

Figure 7. Comparison of modeled [HO_2] from the base model (Br and Cl present; black trace) to simulations performed with only Br (blue trace) and only Cl (red trace) present. Time is expressed in Alaska Standard Time.

ACPD
14, 28685–28755, 2014

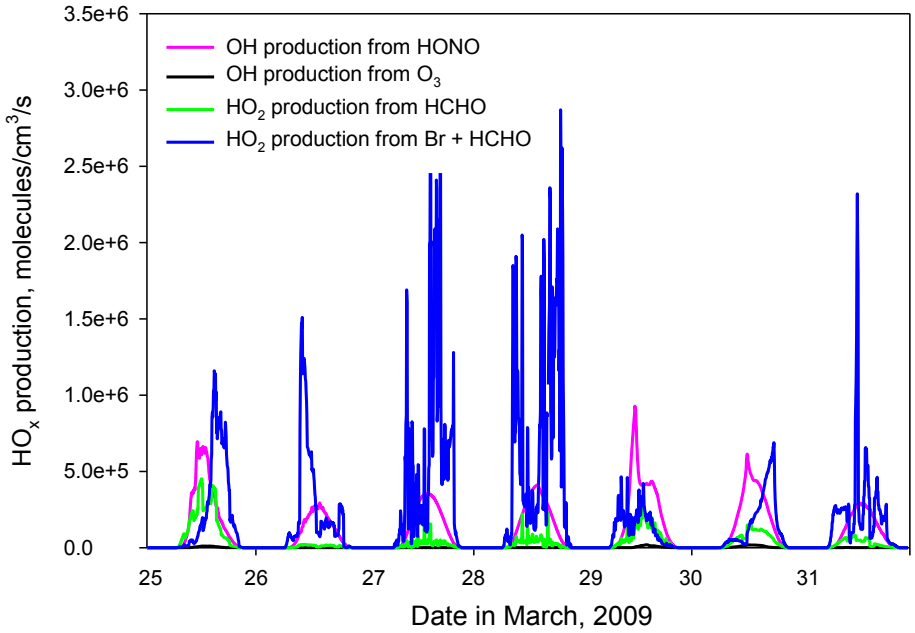

Figure 8. Comparison of HO_x production rates (in molecules $cm^{-3}\,s^{-1}$) for four primary pathways: OH production from HONO photolysis (pink trace), OH production from O_3 photolysis and subsequent reaction with H_2O (black trace), HO_2 production from HCHO photolysis (green trace), and HO_2 production from Br + HCHO reaction (blue trace). Time is expressed in Alaska Standard Time.

ACPD
14, 28685–28755, 2014

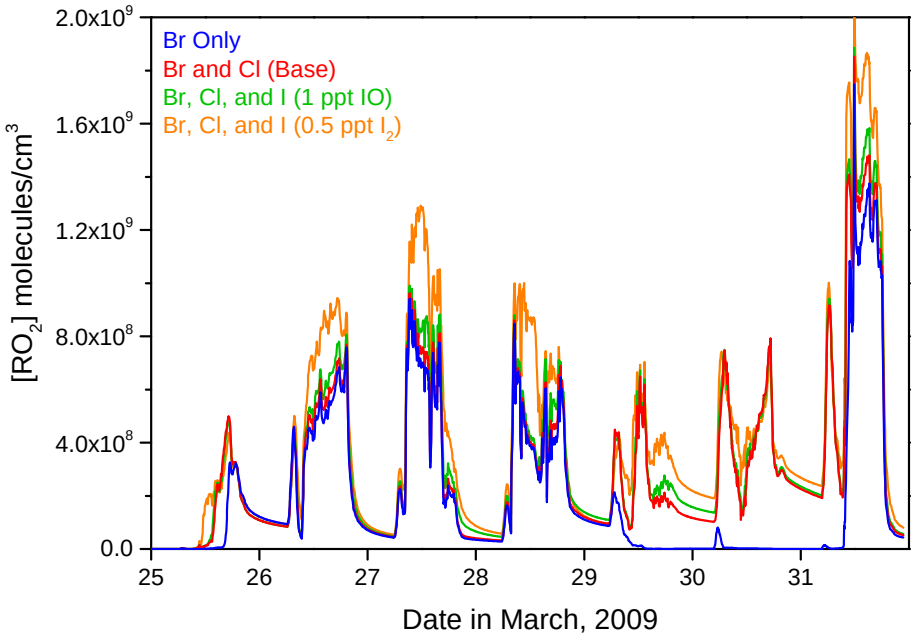

Figure 9. $[RO_2]$ across the 7 day model period, where RO_2 refers to the sum of the methyl through butyl forms of alkyl peroxy radicals. Presented are results from the "Base Model" simulation with Br and Cl present (red trace), a simulation with only Br present (blue trace), a simulation with all three halogen species present (green trace) with 1 pptv IO present, and a simulation with Br, Cl, and I present with I_2 set at 0.5 pptv (approximately 5–6 pptv IO). Time is expressed in Alaska Standard Time.

ACPD
14, 28685–28755, 2014